



저작자표시-비영리-동일조건변경허락 2.0 대한민국

이용자는 아래의 조건을 따르는 경우에 한하여 자유롭게

- 이 저작물을 복제, 배포, 전송, 전시, 공연 및 방송할 수 있습니다.
- 이차적 저작물을 작성할 수 있습니다.

다음과 같은 조건을 따라야 합니다:



저작자표시. 귀하는 원저작자를 표시하여야 합니다.



비영리. 귀하는 이 저작물을 영리 목적으로 이용할 수 없습니다.



동일조건변경허락. 귀하가 이 저작물을 개작, 변형 또는 가공했을 경우에는, 이 저작물과 동일한 이용허락조건하에서만 배포할 수 있습니다.

- 귀하는, 이 저작물의 재이용이나 배포의 경우, 이 저작물에 적용된 이용허락조건을 명확하게 나타내어야 합니다.
- 저작권자로부터 별도의 허가를 받으면 이러한 조건들은 적용되지 않습니다.

저작권법에 따른 이용자의 권리는 위의 내용에 의하여 영향을 받지 않습니다.

이것은 [이용허락규약\(Legal Code\)](#)을 이해하기 쉽게 요약한 것입니다.

[Disclaimer](#)

공학박사학위논문

**Real-time Monitoring and Optimization of
Plasma Etching for Semiconductor
Manufacturing**

반도체 제조를 위한 플라즈마 에칭의 실시간
모니터링 및 최적화

2014년 2월

서울대학교 대학원

화학생물공학부

백 계 현

Abstract

Real-time Monitoring and Optimization of Plasma Etching for Semiconductor Manufacturing

Kye Hyun Baek

School of Chemical & Biological Engineering

The Graduate School of Seoul National University

For several decades, the semiconductor industry has rapidly progressed by the fast paced improvements in its technology. The continuous shrinkage of the chip size makes sub-20nm device era appear, which enables microprocessors with several GHz multiple-core central processing unit and various types of memory devices with several hundred gigabyte capacity. This technology evolution of the industry has been driven by the Moore's law, which has proven to be accurate until the current sub-20nm device era. However, the physical difficulties in materials and patterning technology to cross the 10nm threshold force semiconductor manufacturers to start thinking of more than Moore's law. The concept of more than Moore's law was firstly addressed in 2007, which is the equivalent scaling by

improving the performance of the device, not by shrinking the chip size. Several equivalent scaling approaches are classified into inclusion of process technologies, additional chip and system-level architectural and software design, transition to 450mm wafer, and cost-effective manufacturing through real-time monitoring and control.

Semiconductor manufacturing is composed of various processes such as photo lithography, dry etch, diffusion, ion implantation, thin film deposition, cleaning and chemical mechanical planarization. Among these processes, plasma related processes occupy more than 30% of the whole manufacturing steps. Specifically, plasma etching leads technology evolution in plasma equipment for semiconductor manufacturing.

The cost-effective manufacturing through monitoring and control in plasma etching has been delayed due to the inherent complexity of plasma, lack of plasma sensors, integration issues from deposition and photolithography even though the plasma etching is one of the core processes for semiconductor manufacturing. As a result, the rapid technology development for plasma etch in terms of the cost effective manufacturing is crucial in winning the competitiveness in semiconductor industry.

This thesis has addressed issues in cost effective plasma etch operations and solutions: sensor variable selection and utilization technique, virtual metrology to predict critical dimension, chamber conditioning after wet cleaning, and chamber to chamber matching. All of the developed methodologies were demonstrated in

semiconductor manufacturing environments

Integrated square response based sensor variable selection technique was introduced for handling the scaling issues from various physical properties of sensors in plasma etching and for helping engineers to intuitively select state variables related to manipulate variables. This technique can be integrated with relative gain array and singular value analysis to strengthen its usefulness in plasma etching.

Issues in implementing a robust virtual metrology for plasma etching were discussed: state-of-the art plasma sensors, effective selection of plasma sensor variables responding to individual manipulated variable, sensor data shift across preventive maintenance. In order to handle selection of plasma sensor variables, the integrated square response based sensor selection is refined by the interaction analysis with non-square relative gain array, which can reduce the number of input variables for virtual metrology. With the help of plasma sensor variables and its optimum sensor variable selection, simple linear regression methods such as multiple linear regression and partial least squares regression are successfully applied to predict a metal line critical dimension in plasma etching. The mean absolute percentage error of the virtual metrology systems is less than 5%, which can be maintained by the cost-effective recursive coefficient update technique even under dynamic semiconductor manufacturing environments.

A systematic procedure to optimize chamber seasoning conditions with optical emission spectroscopy was suggested to address the process drift after wet cleaning in plasma etching. In order to achieve a quantitative analysis of plasma spectra without being disturbed by noises from optic systems, a self-background

normalization technique is introduced. Also in order to automatically determine optimum seasoning conditions, a multiple input multiple output control strategy is applied and the optimum condition is obtained by solving the quadratic optimization problems. The suggested methodology was successfully demonstrated in a dynamic random access memory device manufacturing environment which is suffering from a serious process drift after wet cleaning.

The equipment control approach was suggested to solve chamber to chamber performance matching problems. The decomposed etch rate map which enables representation of etch rate profile within a wafer were introduced to design a multiple input multiple output controller with 3 controlled variables. With the 3 controlled variables, the singular value analysis and the relative gain array methods were incorporated with the integrated square response based sensor variable selection technique to find the optimal sets of manipulated variables and controlled variables. In order to find an optimum process condition to match the etch rate performance from the worst to the golden chambers, an optimization problem with constraints was solved. The suggested process condition was applied to the worst chamber, which results in the improvement of the performance matching index from 100.7 to 31.6.

Hopefully, the proposed methodologies in this thesis will be disseminated to semiconductor manufacturers who are experiencing similar issues.

Keywords: Plasma Etching, Variable Selection, Virtual Metrology, Multiple Input Multiple Output Control, Chamber Conditioning, Chamber Matching

Student ID: 2010-30250

Contents

Abstract	i
Contents.....	v
List of Figures	viii
List of Tables.....	x
CHAPTER 1 : Introduction.....	1
1.1. Research motivation.....	1
1.2. Monitoring and optimization in semiconductor manufacturing.....	4
1.3. Research objectives	7
1.4. Outline of the thesis	8
CHAPTER 2 : Sensor Variable Selection and Utilization.....	9
2.1. Introduction.....	9
2.2. Issues in sensor variable selection for plasma etching processes.....	11
2.2.1. Complex multivariate plasma etch process	11
2.2.2. Various sensor variables in plasma etching equipment	14
2.2.3. Scaling sensitive principal component analysis	17
2.3. ISR based sensor variable selection method	22
2.4. Conclusions	28
CHAPTER 3 : Virtual Metrology to Predict Critical Dimension.....	29
3.1. Introduction.....	29
3.2. Considerations on plasma etch-specific VM.....	31
3.2.1. Variable selection with minimum plasma knowledge	31

3.2.2. Sensor data shift across preventive maintenance	32
3.3. Incorporation of ISR based sensor variable selection with RGA method	
34	
3.4. Recursive update algorithm for handling sensor data shift	37
3.5. Results and discussion.....	38
3.5.1. Optimum sensor variable selection for VM	38
3.5.2. Reliable VM system by simple linear regression methods.....	43
3.5.3. Recursive coefficient update to handle sensor data shift.....	45
3.6. Conclusions	49
CHAPTER 4 : Chamber Conditioning after Wet Cleaning	50
4.1. Introduction	50
4.2. Experiment	52
4.3. Issues in wet cleaning for plasma etch systems	53
4.3.1. Serious process drift after wet cleaning.....	53
4.3.2. OES data drift between and across preventive maintenance	56
4.3.3. Optimization problems with OES data.....	61
4.4. Systematic optimization of chamber seasoning conditions.....	65
4.4.1. Step-by-step procedure to optimize chamber seasoning conditions	
through OES	65
4.4.2. Application of step-by-step procedure to Si trench etch process...68	
4.5. Conclusions	72
CHAPTER 5 : Chamber to Chamber Matching by MIMO Controller Design	73
5.1. Introduction	73
5.2. Experiment	75

5.3. Chamber matching issues in semiconductor manufacturing	77
5.3.3. Chamber performance deviations in plasma etching.....	77
5.3.4. Approaches to handling chamber matching issues	82
5.4. Brief theory overview.....	84
5.4.1. Possible MVs and CVs in plasma etching.....	84
5.4.2. Singular value analysis method	86
5.4.3. Dynamic optimization techniques for multiple input multiple output control	87
5.5. Controller development and recipe optimization	88
5.5.1. Design of MIMO controller.....	88
5.5.2. Recipe optimization and chamber performance matching test.....	99
5.5.3. Future aspect for robust chamber matching	105
5.6. Conclusions	105
CHAPTER 6 : Concluding Remarks	107
6.1. Conclusions	107
6.2. Future works.....	109
Nomenclature	110
Literature cited	115
Abstract in Korean (요약).....	124

List of Figures

Figure 2-1. Overview of a complex multivariable plasma etch process whose variables are classified into MVs, SVs, and PVs.	13
Figure 2-2. Schematic of a plasma etching system and additional in-situ sensors..	16
Figure 2-3. Loadings of the first PC without data normalization.	19
Figure 2-4. Loadings of the first PC with mean centered data normalization.	20
Figure 2-5. Loadings of the first PC with mean centered and unit variance data normalization.	21
Figure 2-6. Signals of collision rate for the step change test of source power: (a) raw signal of collision rate and (b) normalized signal.	27
Figure 3-1. CD and plasma sensors behavior across PM.	33
Figure 3-2. Metal line CD prediction performance of VM systems: (a) MLR and (b) PLSR are applied to build the VM model.	44
Figure 3-3. Metal line CD prediction performance of PLS based VM systems without the recursive coefficient update technique.	47
Figure 3-4. Metal line CD prediction performance of PLS based VM system with the recursive coefficient update technique.	48
Figure 4-1. Si etch rate trend after wet cleaning.	54
Figure 4-2. OES spectra over different wafers (non-pattern Si wafer and production wafer) with the same plasma condition.	55
Figure 4-3. Spectral changes with time during a PM period.	58
Figure 4-4. Raw spectra of different wafers with the same recipe.	59

Figure 4-5. Normalized spectra of a production wafer and NPW showing the big different wavelength positions in terms of intensity.....	60
Figure 4-6. Comparison of normalized OES spectra between production and NPWs.	63
Figure 4-7. Empirical model space of 3 factor Box-Behnken design.	64
Figure 4-8. A process flow for optimization of a chamber seasoning condition.	67
Figure 4-9. Comparison of the normalized spectra around CV in each plasma.	71
Figure 5-1. Schematic of CCP reactor employed in this chapter.....	76
Figure 5-2. Performance differences between the golden chamber (best product yield) and other chambers in terms of etch rate maps.	79
Figure 5-3. Etch rate differences between the golden chamber (best product yield) and other chambers in A-A' direction indicated in figure 5-2.	80
Figure 5-4. Performance distribution of chambers over time.....	81
Figure 5-5. Possible procedure to handle chamber matching issues.	83
Figure 5-6. Decomposed etch rate map with four directions.	92
Figure 5-7. Difference of etch rate performance according to four directions in figure 5-6 between the golden and the bed chambers.	93
Figure 5-8. Confirmation results with the optimized condition from the second set of MVs (directions refer to figure 5-6) with PMI=31.6	104

List of Tables

Table 2-1. List of sensor variables employed in this chapter.....	15
Table 2-2. Step change test conditions of seven MVs for sensor data acquisition..	25
Table 2-3. Top 10 sensor variables based on ISR with regard to source power, bias power, and gas 4 flow.....	26
Table 3-1. The calculated NRGAs of the (18 x 7) steady-state gain matrix	41
Table 3-2. The top 10 square sub-systems having lowest SSEs	42
Table 4-1. Experimental design for the Box-Behnken design for an OES to MVs model.....	66
Table 4-2. Suggested MV settings from the optimization problems.	69
Table 4-3. Comparison of Si etch rate according to different plasma conditions....	70
Table 5-1. Typical process variables in plasma etching.	85
Table 5-2. PMI for each chamber (chamber 3 was the worst chamber).	91
Table 5-3. Raw gain matrix with 6 MVs and 5 CVs.	96
Table 5-4. CN values with MVs and CVs for (a) 4 x 4 matrix and (b) 3 x 3 matrix after SVA.	97
Table 5-5. RGA results with 5 top ranked MVs and CVs set in Table 5-4 (raw gain)	98
Table 5-6. Constraints for each MV.....	101
Table 5-7. Prediction error for three control strategies.....	102
Table 5-8. Optimized values for each MV according to control strategy.	103

CHAPTER 1 : Introduction

1.1. Research motivation

For several decades, the semiconductor industry has rapidly progressed by the fast paced improvements in its technology. The continuous shrinkage of the chip size makes sub-20nm device era appear, which enables microprocessors with several GHz multiple-core central processing unit (CPU) and various types of memory devices with several hundred gigabyte capacity. This technology evolution of the industry has been driven by the Moore's law which was firstly suggested by Gordon E. Moore in 1965.^[1] His prediction that the number of transistors on integrated circuits will double approximately every two years has proven to be accurate until the current sub-20nm device era. However, the physical difficulties in materials and patterning technology to cross the 10nm threshold force semiconductor manufacturers to start to think of more than Moore's law. The concept of more than Moore's law was firstly addressed in 2007 by the ITRS, which is the equivalent scaling by improving the performance of the device, not by shrinking the chip size.^[2]

Several equivalent scaling approaches are classified into inclusion of process technologies, additional chip and system-level architectural and software design, transition to 450mm wafer, and cost-effective manufacturing through real-time monitoring and control. The inclusion of process technologies contains gate strain in the channel, High-K metal gate materials in the transistor gate, transistor 3D architecture called fin shaped field effect transistor (FinFET), and new channel

materials like III/V compounds and so on. The additional chip and system-level architectural and software design includes SRAM memory architecture, CPU multiple-core, power software management enabled the chips etc. The transition to 450mm diameter wafer is another enabler for more than Moore's law. The need for 450mm wafer generation transition has been emphasized since 2007 by the International Semiconductor Manufacturing Technology Manufacturing Initiative (ISMI). Major players in semiconductor manufacturing such as Intel, Samsung, and TSMC announced in May 2008 that they would work together with suppliers, other semiconductor players, and ISMI to develop 450mm pilot line in 2012. Finally, the cost-effective manufacturing through monitoring and control has been made for several decades in various industries. The core strategy that is to do business safely and efficiently has been differentiated, depending on the industries. In the semiconductor industry, advanced equipment control and advanced process control (AEC/APC) conferences are held in three different continents like US, Europe, and Asia, which is an annual event to share their own advancement.

Semiconductor manufacturing is composed of various processes such as photo lithography, dry etch, diffusion, ion implantation, thin film deposition, cleaning, and chemical mechanical planarization. Among these processes, plasma related processes occupy more than 30% of the whole manufacturing steps. Specifically, plasma etching leads technology evolution in plasma equipment for semiconductor manufacturing.

The cost-effective manufacturing through monitoring and control in plasma etching has been delayed due to the inherent complexity of plasma, lack of plasma sensors, integration issues from deposition and photolithography even though the

plasma etching is one of the core processes for semiconductor manufacturing. As a result, the rapid technology development for plasma etch in terms of the cost effective manufacturing is crucial in winning the competitiveness in semiconductor industry.

1.2. Monitoring and optimization in semiconductor manufacturing*

The semiconductor manufacturing is a capital-intensive industry, in which the cost of building a new fab is estimated to be over several billion U.S. dollars. Advances in semiconductor device technologies typically require additional investments to upgrade manufacturing equipment. The rapid shrinkage of the semiconductor device drives manufacturing equipment to be equipped with more precise capabilities so that equipment can meet process performance targets under a tight process window.

Owing to the capital intensity and the required capability for a tight process window, it is crucial to maintain highly efficient operations with monitoring and control capability in semiconductor manufacturing. Typically a modern fab has three typical measurements: real time data at the tool level which reflect the equipment health condition, in-line metrology data to measure geometric dimensions after a major processing step, and simple and final electrical test data available for electrical properties with medium or long time delay.^[3]

The real time data at the tool level such as temperature, pressures and gas flow rates are used to monitor recipes applied to single wafers or batches of wafers.^[4] Some typical processing operations include plasma etching, thin film deposition, rapid thermal annealing, ion implantation, and chemical mechanical planarization. At most processing steps, sensors collect data for each wafer or batch of wafers that are processed on the tool. This data can be in the form of real time data for a

* The partial part of this chapter is taken from the author's published papers.^[3,4]

recipe, summary statistics available at the end of each run or data from more advanced sensor platforms such as optical emission spectroscopy (OES).

Data based fault detection and diagnosis has been successfully developed and applied in other industries.^[5, 6] These data driven fault detection techniques are based on multivariate statistical analysis such as principal component analysis (PCA) and partial least squares (PLS) and are related to statistical quality control methods.^[7, 8]

While the batch nature of semiconductor manufacturing provides plenty of opportunities for applying multi-way process monitoring,^[9] many forms of semiconductor metrology data are naturally organized in three dimensions. Multi-way PCA has been successfully applied for batch process monitoring across many different industries. In the field of semiconductor manufacturing, the concept of unfolding data was demonstrated by applying multi-way PCA to OES for plasma etchers.^[10]

The in-line metrology data are normally gathered at several locations on the semiconductor wafers, oftentimes for multiple features at the same site. These are top and bottom critical dimensions. Fault detection and identification applied to site-level metrology data is intended to validate whether the structures built on the semiconductor wafers hit their targets and do so uniformly across the wafer surfaces. The transition from 200mm to 300mm technology and beyond makes it possible to replace in-line metrology with integrated metrology into the tools. The integrated metrology reduces the time delay in the measurement and provides the possibility of wafer to wafer control which can reduce the variability further. Another possibility is within wafer control that allows one to control from die to

die.^[11] The integrated metrology with 300mm fabs provides fast and timely measurement for control, but it may not be necessary or cost-effective to sample at every wafer. An optimal and adaptive sampling plan that will reduce the sampling cost without sacrificing control accuracy was presented.^[11] In addition wireless metrology can provide an ample opportunity for advanced monitoring and control.^[12]

To implement the fab-wide control, it is important to develop a physics-based device model that maps geometric parameters to electrical parameters such as oscillation frequency, erase time of flash memories, and sheet resistance. This model is different from process models used in run-to-run controllers that describe the relation between process operation conditions to geometric parameters such as critical dimensions, depth, or thickness. Since optimization is involved in electrical parameter control (EPC), which could use the model in fairly wide operation regions, nonlinear physics based models are appropriate for this task. The model suitable for EPC must be implementable in real time, making it different from simulation and design models such as technology computer aided design (TCAD) models. Model reduction is therefore an important issue for EPC. As the semiconductor industry progresses into sub 20nanometers, multi-scale modeling and simulation become important. These models^[13, 14] can help understand the microscopic behavior and avoid potential defect by effective control. It is possible that equation-free simulation models^[15] could be used for control and constraint handling.

1.3. Research objectives

The objective of the thesis is to suggest systematic methodologies to implement cost-effective manufacturing in plasma etching through effective utilization of plasma sensors and computational optimization. Since intensive process integration knowledge is required in addition to the sophisticated knowledge for plasma, plasma etching engineers have difficulties in optimizing their processes. In order to enable them to do their jobs effectively, additional plasma sensors monitoring plasma states and their effective utilization should be continually developed. Furthermore, plasma knowledge should be more formularized so that engineers can afford to apply it. For this purpose, a methodology to intuitively utilize plasma sensor variables will be suggested for effective sensor variable selection as a starting point. Together with the optimum variable selection methodology, process optimization techniques for cost-effective plasma etching operation will be demonstrated in a semiconductor manufacturing environment so that the cost-effective manufacturing through monitoring and optimization can be implemented in plasma etching areas.

1.4. Outline of the thesis

The thesis is organized as follows. Chapter 1 suggests an explanation about motivation, monitoring and optimization trend in semiconductor manufacturing, and objectives of the research as introduction. As a starting point of the effective operation of plasma etching processes, a sensor variable selection and utilization technique is described in Chapter 2. It follows by the development of the virtual metrology (VM) to predict metal line critical dimension (CD) in Chapter 3. From Chapter 4 to Chapter 5, chronic issues in plasma etching which disturbs cost-effective operations in plasma etch system for semiconductor manufacturing will be handled. Systematic optimization of chamber seasoning conditions by using optical emission spectroscopy (OES) will be introduced in Chapter 4. This is enabled by the development of a signal normalization technique for quantitative analysis of OES. In addition, optimization problems with constraints are done by the computational power in order to obtain the optimum condition automatically. In Chapter 5, an equipment control approach to covering chamber to chamber matching issues will be discussed, which contains methodologies for designing an optimum multiple input multiple output (MIMO) controller for a plasma etch control. This thesis will conclude the summary of the results which were demonstrated in semiconductor manufacturing environments and the outline for future work.

CHAPTER 2 : Sensor Variable Selection and Utilization

2.1. Introduction

In today's semiconductor manufacturing environment, many in-situ sensors are employed for monitoring plasma etch equipment operation and process results due to the inherent complexity of plasmas.^[10, 16-20] The potential number of measurements in plasma etching is greater than several hundred. Despite the large number of existing sensors, process and equipment engineers in plasma processing continue to evaluate newly developed state-of-the-art sensors because they believe that current sensors do not provide enough information about plasma states. Therefore, the number of in-situ sensors in plasma processes is expected to increase, which provides an incentive to develop an effective procedure for sensor variable selection and utilization.

Because plasma etch processes are complex multivariable processes, manipulated variables (MVs) can be adjusted considering state variables (SVs) and performance variables (PVs). Since SVs measure hardware and plasma states through various in-situ sensors, their proper utilization is invaluable for process set-up, process and equipment control, and fault detection. However, utilization of SVs in practice is limited because interpretation of them regarding MVs and PVs requires additional knowledge. Therefore, a general and efficient approach to selecting proper SVs and their utilization needs to be developed.

This chapter discusses an effective procedure for sensor variable selection and

utilization in plasma etching. Firstly, several issues in sensor variable selection for plasma etching will be addressed in terms of complexities of plasma etch processes, variety of in-situ sensors and scaling issues. Then, a brief theory overview which is suggested in this thesis will be made. The proposed sensor variable selection technique can be utilized as a starting point in building a reference sensor library for fault detection and classification, evaluating sensor performance, and selecting MVs – PVs for equipment control.

2.2. Issues in sensor variable selection for plasma etching processes

2.2.1. Complex multivariate plasma etch process

Plasma etching is a key process together with photolithography for patterning in semiconductor manufacturing.^[21] This process uses plasma to generate highly reactive ionized species from relatively inert molecular gases to remove material from surfaces. The ionized species are accelerated in a perpendicular direction to wafer by the sheath potential of the plasma, which enables performing anisotropic etching processes. However, the plasma etch processes are complicated due to the inherent complexity of plasmas. That is, in addition to the physical and chemical reactions in plasma etching, the electrical interaction between charged particles and the electromagnetic fields within the plasma, which can be reflected to plasma state variables from plasma sensors, are not simple to interpret. Therefore, plasma etch processes must consider plasma state variables together with input and output variables to better understand their processes.

Figure 2-1 illustrates the three groups of variables in a plasma etch process, where the plasma is a medium connecting MVs and PVs with several hundred SVs. Until recent years, a group of equipment state variables from built-in hardware gauges have been mainly utilized for equipment monitoring and process readiness check. However, with the narrower process window due to the semiconductor device shrinkage, the detection capability of those SVs is now insufficient to measure process performance. As a result, plasma state variables from plasma sensors, which are more representative of process results, are emerging as alternatives.

Utilization of plasma state variables, however, is limited because it requires additional knowledge to interpret in terms of their relationships to MVs and PVs. In addition, the limited number of plasma sensors currently available in an industrial environment makes this situation worse because of the lack of information on the plasma. Therefore, the number of new plasma sensors will continue to increase and with the increased number, an efficient and affordable sensor variable selection and utilization technique needs to be developed in plasma etch processes.

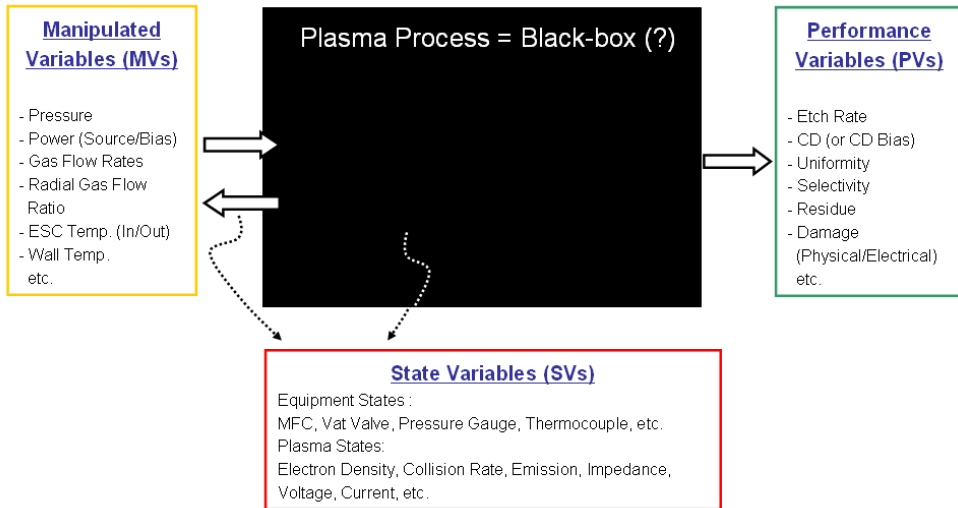


Figure 2-1. Overview of a complex multivariable plasma etch process whose variables are classified into MVs, SVs, and PVs.

2.2.2. Various sensor variables in plasma etching equipment

The schematic of the plasma etching equipment and additional in-situ sensors employed in this chapter is shown in Fig. 2-2. The etching equipment is an inductively coupled plasma reactor from Applied Materials, Inc., which uses the RF power of 13.56MHz to generate plasma through inductive coupling and has optical emission spectroscopy (OES) and VI-probe built in the equipment. The OES sensor measures emission spectra ranging from 200nm to 800nm, which reflects chemical properties in plasma.^[22] The VI-probe sensor measures the voltage, current and phase of the RF power of 13.56MHz and its harmonics, with which the sheath potential of plasma can be estimated.^[23] The self-excited electron resonance spectroscopy (SEERS) from Plasmetrex GmbH is an additionally installed sensor, which measures electrical and chemical properties of the plasmas such as electron density, and electron collision rate, and so on.^[16, 18, 24] The other sensors that monitor equipment states like pressure and temperature are not shown in Fig. 2-2, but they are also evaluated together.

Table 2-1 lists sensor variable categories employed in this paper, which shows the total number of sensor variables is 1,308 and each sensor variable has the different physical properties. As discussed in section 2.2.1, the total number of sensor variables in plasma etching has been continually growing, so their proper utilization will be difficult if effective variable selection techniques do not exist.

Table 2-1. List of sensor variables employed in this chapter.

Hardware Gauges		SEERS		VI-probe		OES	
Variables	Description	Variables	Description	Variables	Description	Variables	Description
Throttle current_pct_open	Throttle valve open level	Collision rate	Electron collision rate	f0V	Fundamental voltage	200.0nm	Emission intensity
Source forward_reading	Forward power reading	Electron density	Electron density	f0I	Fundamental current	200.5nm	Emission intensity
Source reflected_reading	Reflected power reading	1 st Harmonics	1 st harmonics current	f0Phase	Fundamental phase	201.0nm	Emission intensity
Source series_reading	Matchbox reading (Series Cap.)	2 nd Harmonics	2 nd harmonics current	f1V	1 st harmonics voltage	201.5nm	Emission intensity
Source shunt_reading	Matchbox reading (Shunt Cap.)	3 rd Harmonics	3 rd harmonics current	f1I	1 st harmonics current	.	.
Source div cap_current_1	Current flowing source coil1	4 th Harmonics	4 th harmonics current	f1Phase	1 st harmonics phase	.	.
Source div cap_current_2	Current flowing source coil2	2 nd phase	2 nd harmonics current	f2V	2 nd harmonics voltage	.	.
.	.	3 rd phase	3 rd harmonics phase	f2I	2 nd harmonics current		
.	.	4 th phase	4 th harmonics phase	f2Phase	2 nd harmonics phase		
.	.			f3V	3 rd harmonics voltage		
				f3I	3 rd harmonics current		
				f3Phase	3 rd harmonics phase		
				f4V	4 th harmonics voltage		
				f4I	4 th harmonics current		
				f4Phase	4 th harmonics phase		
				f5V	5 th harmonics voltage		
				f5I	5 th harmonics current		
				f5Phase	5 th harmonics phase		
80		9		18		1201	

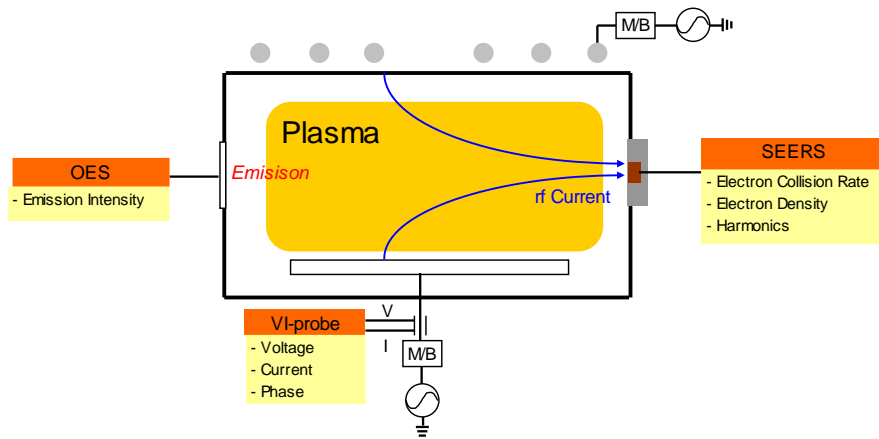


Figure 2-2. Schematic of a plasma etching system and additional in-situ sensors.

2.2.3. Scaling sensitive principal component analysis

Principal component analysis (PCA) is a mathematical procedure that uses orthogonal transformation. It converts a set of observations of possible correlated variables into a set of values of linearly uncorrelated variables called principal components.^[25, 26] This transformation is defined in such a way that the first principal component accounts for as much of the variability in the data as possible and each subsequent component in turn has the highest variance possible under the constraint that it should be orthogonal to the preceding components. Often, its operation can be thought of as revealing the internal structure of the data in a way that best explains the variance in the data. Thus the loading of the first principal component (PC) can be analyzed in terms of importance of sensor variables which accounts for the variability of the data set.

PCA is sensitive to the scaling of the variables. This might lead to arbitrary decision of sensor selection in plasma etching where more than hundreds sensor variables with different physical properties exist like that shown in Table 2-1. Figures 2-3 to 2-5 illustrate how the weightings of each sensor variables in the loading vector of the first PC are changing according to the data normalization methods in plasma etching. For example, the negatively or positively highest weighting sensor variable is changed from sensor variable number 250 in the no-scale case into sensor variable number 122 in the mean centered case, or into sensor variable number 100 in the mean centered and unit variance case. Therefore, unless any additional techniques about scaling is built in PCA to handle the scaling issue, the statistic based PCA cannot be applied to sensor variable selection in plasma etching. In addition, relying on the statistics without considering physical

properties of sensor variables may lead to a wrong decision in plasma etching where nonlinear behavior of plasma governs reaction of process. Thus an affordable sensor variable selection technique which can reflect physical properties of sensor variables and analyze the interaction between variables within plasma needs to be developed in plasma etching processes.

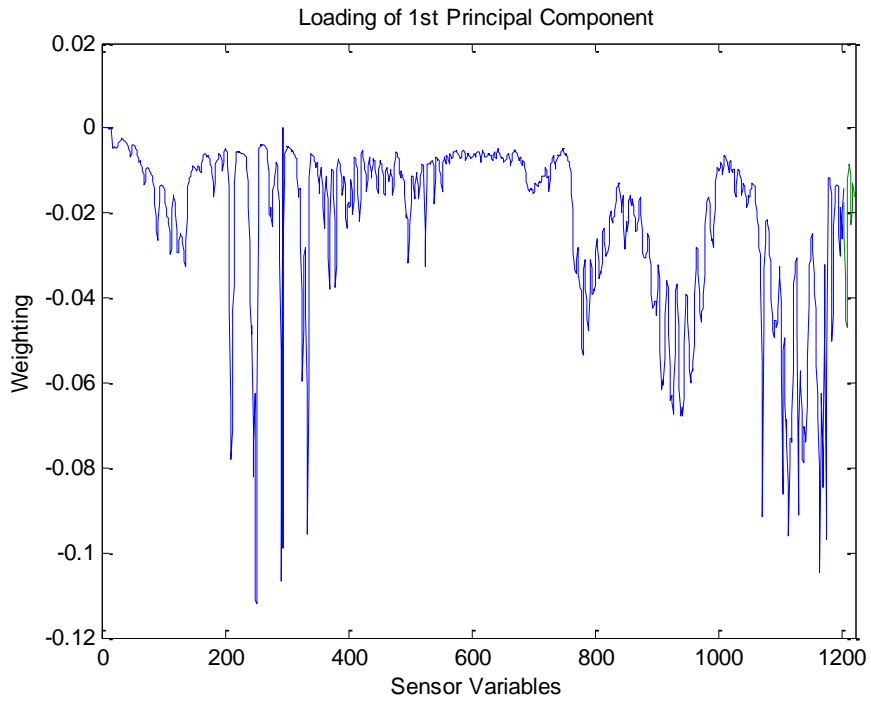


Figure 2-3. Loadings of the first PC without data normalization.

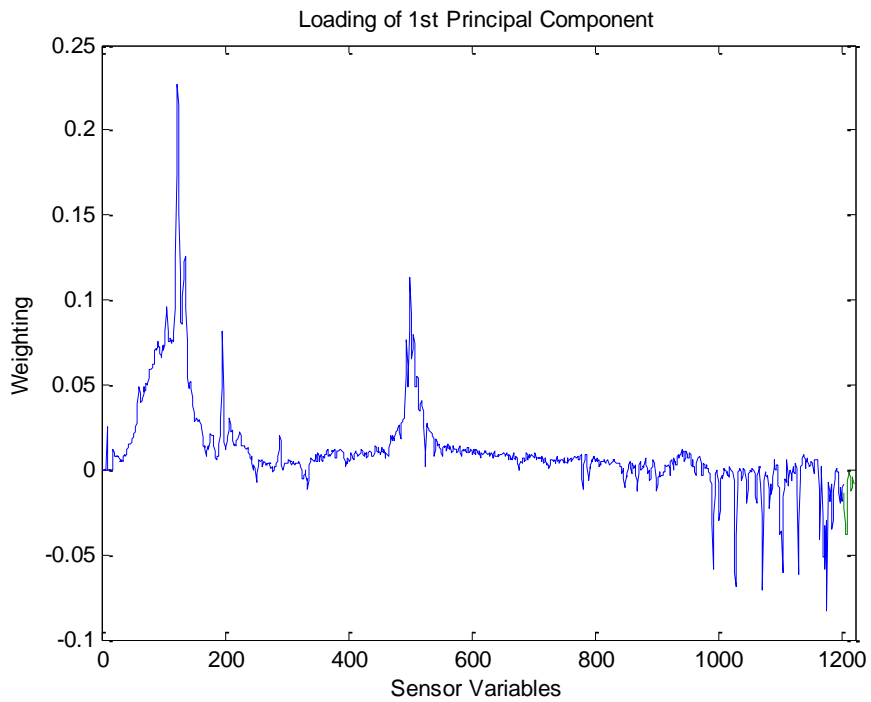


Figure 2-4. Loadings of the first PC with mean centered data normalization.

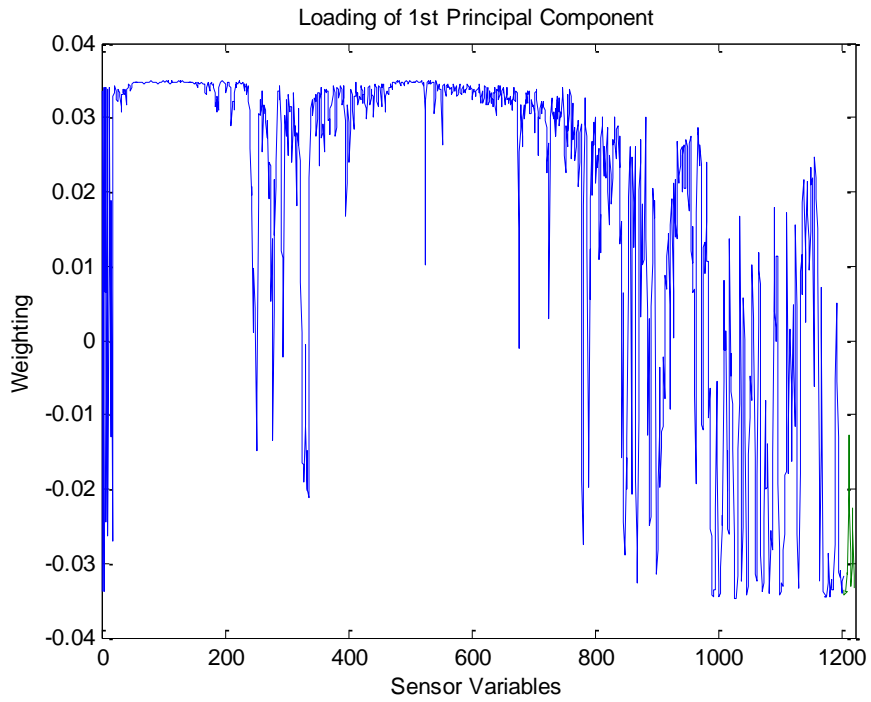


Figure 2-5. Loadings of the first PC with mean centered and unit variance data normalization.

2.3. ISR based sensor variable selection method

Under the consideration of the circumstances in sensor variable selection described in section 2.2, several factors should be taken into account in plasma etching. The first factor is the heterogeneity of SVs. This comes from various sensors to measure plasma characteristics and equipment states as well and might cause scaling issues of variables due to the different unit and sensitivity of each sensor variable. The second factor is the redundancy in the data. This might cause the collinearity issues which lead to numerical instabilities in calculation and poor prediction performance in regression modeling. The third factor is the presence of interactions and non-linearities among SVs due to the inherent complexity of the plasmas. Therefore, a new variable selection method for plasma etching processes should be developed in such a way to minimize the bad effects from the factors above.

A sensor variable ranking table, which sorts all sensor variables in a descending order in terms of each MV, would be useful as a starting point in variable selection. This is because the process results in plasma etching are closely related to SVs and SVs are manipulated by MVs. The sensor variable ranking table should be obtained after the entire sensor responses to each MV are analyzed, which takes large amount of time and knowledge. Given this situation, a systematic procedure to collect and analyze the entire sensor responses would be desirable.

As a systematic procedure for sensor data collection and analysis, a time-integrated variance calculation method with a step change test is suggested. By running the one recipe like that summarized in Table 2-2, the entire sensor response data for each MV can be collected at one time. To make sure that each step change

test is done on the same condition, a step with the baseline condition before and after the step change test is inserted. The step time is determined long enough to reach steady state, which is monitored by plasma parameters such as electron collision rate and electron density from SEERS.

Since each steady state sensor response shows strong, moderate or weak response to the step change of MVs, a numerical criterion, integrated square response (ISR), is developed for their classification. Figure 2-6 shows how ISR is calculated from a raw sensor signal after a step change test. The raw signal of collision rate from SEERS, which measures electron collision frequency in plasma, shows significant response to a 10% change of source power at 46 seconds and reaches steady state in a few seconds. The raw signal of collision rate is then normalized by using Eq. 2-1.

$$y^* = \frac{(y_+(t) - y_{ss})}{y_{ss}} \quad (2-1)$$

This normalization by Eq. 2-1 solves scaling issues in plasma etching, which is described in section 2.2.3 and the first paragraph of section 2.3. The normalized data, y^* , are then integrated from the start to the end of the step change for the ISR calculation:

$$ISR = \frac{1}{b-a} \int_a^b (y^*(t))^2 dt \quad (2-2)$$

Table 2-3 lists a part of sensor variable ranking table for source power, bias power, and flow rate of Gas 4, based on ISR. For source power, two variables from SEERS, six variables from OES, one variable from VI-probe, and one variable from the hardware gauge group are selected as the top ten important sensor

variables. This result is thought to be reasonable, given that all of the selected variables are related to the properties of electron, ion and etchant in the plasma. Specifically, collision rate from SEERS has a great sensitivity of 588.30% for 10% step change of source power. In addition, E-chuck current has a good sensitivity of 70.26% for the same step change of source power. In the bias power case, five variables from SEERS, three variables from VI-probe, and two variables from hardware gauges are selected, but no variables from OES are included in the list. This result is also plausible, given that bias power does not impact etchant very much and both VI-probe and the selected hardware gauges measure RF properties of bias power. As the similar result to source power case, collision rate from SEERS shows the most sensitive response against other sensor variables (59.57%). This implies that bias power affects plasma characteristics in the process condition regime. For the flow rate of Gas 4, eight variables from OES and two variables from SEERS are in the top ten sensor variable list. This is also thought to be a reasonable result, given that OES and SEERS can measure chemical properties of plasma that is changed by increasing gas flow rate. When it comes to the sensitivity of sensor variable response, OES does not play important role, which is indicated in its response values. Therefore, additional sensors with an acceptable sensitivity should be developed in the gas 4 flow case. By considering the interpretation, it is thought that sensor ranking based on ISR reflects intuitive physical and chemical properties of sensor variables.

Table 2-2. Step change test conditions of seven MVs for sensor data acquisition.

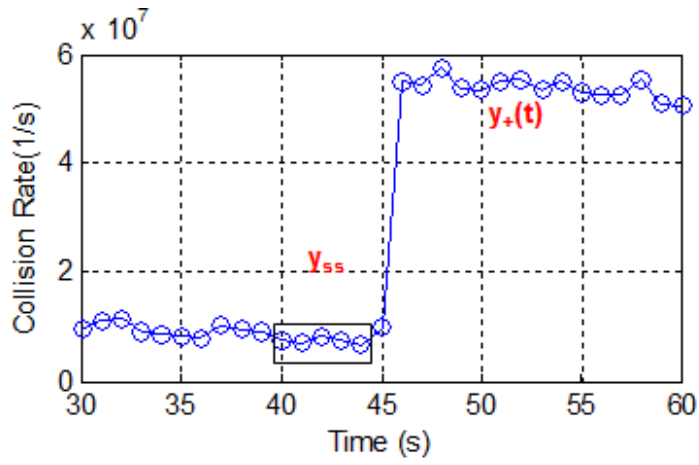
MVs	1 st Step	2 nd Step	3 rd Step	4 th Step	5 th Step	6 th Step	7 th Step	8 th Step	9 th Step	10 th Step	11 th Step	12 th Step	13 th Step	14 th Step	15 th Step
Pressure			10% Up		Base										
Source Power					10% Up		Base			Base					
Bias Power							15% Up				Base			Base	
Gas1 Flow	Stable	Base		Base		Base		Base		10% Up	Base		Base		Base
Gas2 Flow			Base		Base							10% Up			
Gas3 Flow									Base					10% Up	
Gas4 Flow													Base		10% Up

Note: Base means setting for each parameter is a baseline condition.

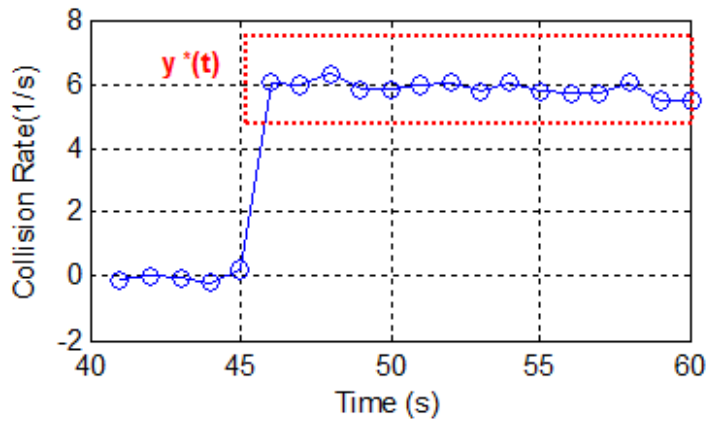
Table 2-3. Top 10 sensor variables based on ISR with regard to source power, bias power, and gas 4 flow.

	Source Power	ISR/ Response ¹	Bias Power	ISR/ Response ¹	Gas 4 Flow	ISR/ Response ¹
1	Collision Rate	3.461x10/ 588.30%	Collision Rate	3.549x10 ⁻¹ / 59.57%	Collision Rate	1.063x10 ⁻¹ / 32.60%
2	E-chuck Current	4.936x10 ⁻¹ / 70.26%	4 th Harmonics	5.040x10 ⁻² / 22.45%	Electron Density	3.713x10 ⁻⁴ / 1.93%
3	4 th Harmonics	1.444x10 ⁻² / 12.02%	f2V	3.936x10 ⁻² / 19.84%	OES 7	3.155x10 ⁻⁴ / 1.78%
4	OES 1	1.346x10 ⁻² / 11.60%	f1V	2.097x10 ⁻² / 14.48%	OES 8	1.342x10 ⁻⁴ / 1.16%
5	OES 2	1.156x10 ⁻² / 10.75%	DC Bias	2.097x10 ⁻² / 14.48%	OES 9	1.234x10 ⁻⁴ / 1.11%
6	OES 3	1.143x10 ⁻² / 10.69%	2 nd Harmonics	1.457x10 ⁻² / 12.07%	OES10	1.229x10 ⁻⁴ / 1.11%
7	OES 4	1.142x10 ⁻² / 10.68%	Peak Voltage	1.045x10 ⁻² / 10.22%	OES 1	1.207x10 ⁻⁴ / 1.10%
8	OES 5	1.075x10 ⁻² / 10.37%	3 rd Harmonics	9.763x10 ⁻³ / 9.88%	OES11	1.161x10 ⁻⁴ / 1.08%
9	f0V	1.022x10 ⁻² / 10.11%	1 st Harmonics	7.347x10 ⁻³ / 8.57%	OES12	1.142x10 ⁻⁴ / 1.07%
10	OES 6	9.968x10 ⁻³ / 9.98%	f4V	5.878x10 ⁻³ / 7.67%	OES13	1.130x10 ⁻⁴ / 1.06%

¹Response: square root of ISR



(a)



(b)

Figure 2-6. Signals of collision rate for the step change test of source power: (a) raw signal of collision rate and (b) normalized signal.

2.4. Conclusions

Because plasma etching processes have a large number of SVs to be utilized, and the number of possible SVs is continually growing, an effective sensor variable selection technique is necessary. The time-integrated variance calculation method introduced in this chapter can be a proper approach to handling a large number of sensors. Based on ISR obtained through the time-integrated variance calculation of sensor data from step change tests, sensor variables can be ranked with regard to particular MVs, which can be utilized to make ISR-based sensor variable tables. With the ISR-based sensor variable tables, process and equipment engineers can gain insight into physical behavior of complicated plasma sensors. In addition, the ISR-based sensor variable tables can be integrated with relative gain array (RGA) and singular value analysis (SVA) in selecting optimum variable selection for plasma etch control, which will be introduced in Chapter 3 and 5.

CHAPTER 3 : Virtual Metrology to Predict Critical Dimension

3.1. Introduction

Virtual metrology (VM) is a technique to estimate wafer metrology variables using in-situ sensor measurements, where is a regression model between SVs as input and PVs as output. Due to its ability to provide wafer-to-wafer quality assurance, VM has been attracting much interest in recent years from semiconductor manufacturer researchers.^[27-34] A well-developed VM system can reduce requirements for physical metrology, which is expensive and is a bottleneck in semiconductor manufacturing. VM provides real-time quality assurance for production tools instead of scheduled tool monitoring with test wafers. In addition, VM can be incorporated into wafer-to-wafer process control strategies, which can mitigate measurement delay issues.^[28, 35]

Building a VM system in plasma etching starts from input variable selection for an output variable such as critical dimension (CD), etch depth, or etch rate. However, since plasma etch processes have a large number of in-situ sensors due to the inherent complexity of plasmas.^[10, 16-20, 22, 23], selecting proper input variables that are better correlated with output variables is always challenging when implementing a reliable VM system.

The plasma etching environment in semiconductor manufacturing is dynamic due to various products and equipment variability. From the equipment variability perspective, equipment aging characteristics are equipment-specific so that

scheduled preventive maintenance (PM) maintains the equipment performance within desired targets. Wet cleaning, one of the major PMs, can cause many changes in equipment states because major inside parts are swapped with pre-cleaned parts to save time. The parts swapping impact can be detected clearly by plasma sensors but it is less reflected in process results. These different responses between sensor data and process results across PM require cost-effective adaptation techniques to achieve reliable VM performance.

This chapter discusses implementing robust VM for plasma etching. For this purpose, several considerations in plasma etching for building a VM system will be addressed in section 3.2. Then, methodologies to handle those considerations will be briefly introduced in section 3.3 and 3.4. In section 3.5, demonstration of the introduced methodologies in manufacturing a dynamic random access memory will be shown, which proves the effectiveness of these methodologies.

3.2. Considerations on plasma etch-specific VM

3.2.1. Variable selection with minimum plasma knowledge

The number of in-situ sensors employed in plasma etch equipment is potentially more than several hundred. In addition to the huge number of sensor variables in plasma etching, utilization of sensor variables is limited because it requires additional knowledge to interpret in terms of their relationships to MVs and PVs. Specifically, plasma sensors are difficult to utilize because they require high-level knowledge of the plasma. Thus an efficient and affordable sensor variable selection technique needs to be developed in plasma etching.

Building a VM system for plasma etching starts from input variable selection for each output variable (e.g., CD, etched depth, or etch rate). However, since plasma etch processes have a large number of SVs from sensors as described in the previous paragraph, selecting proper input variables that are better correlated with output variables is always challenging when implementing a reliable VM system. In addition, the number of selected input variables should be minimized, given that the cost for computer resources to maintain a fab-wide VM system can increase with the number of input variables. Therefore, variable selection is an important step in building a VM system. For this reason, many statistical approaches have been tried for variable selection.^[31, 35-38] Those statistical approaches may be useful in handling a large number of variables, but relying solely on statistical methods without consideration of the physical meanings of variables may exclude important variables. In addition, the result that a VM system in plasma etching shows much more reliable performance by selecting important plasma variables^[39]

underscores the consideration of physical properties on variables in selecting input variables. Under these circumstances, a new variable selection approach that can reflect physical meaning of variables or engineers' knowledge is valuable for a reliable and cost-effective VM system.

3.2.2. Sensor data shift across preventive maintenance

One of the major PM events in semiconductor manufacturing is wet cleaning, which can cause many changes in equipment states because major internal parts are replaced with new or pre-cleaned parts. The parts replacement can be detected clearly by plasma sensors but it is less reflected in process results, such as shown in Fig. 3-1. Although the actual CD shows no distinction, sudden shift of the plasma sensor data across PM result in poor CD prediction performance. These different responses between plasma sensor data and process results across PM require adaptation techniques to achieve reliable VM performance.

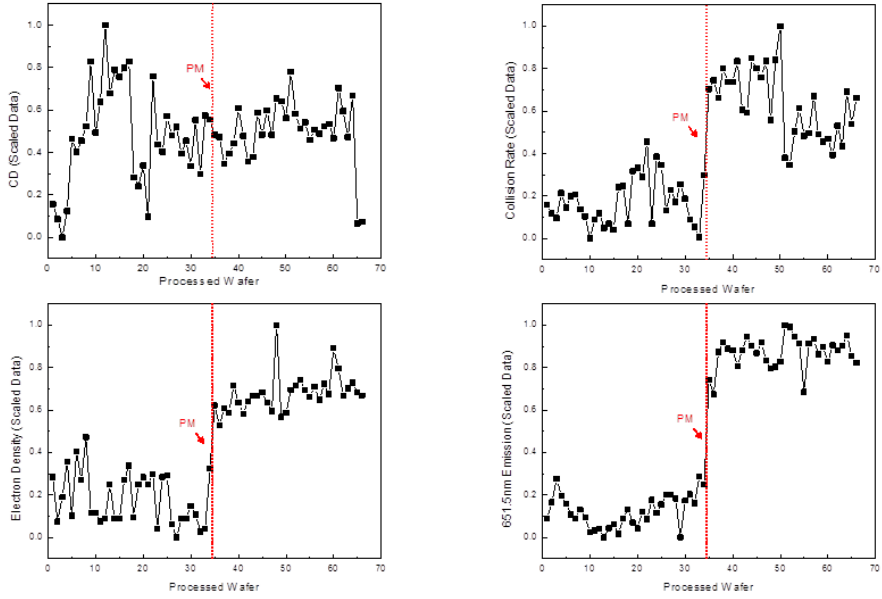


Figure 3-1. CD and plasma sensors behavior across PM.

3.3. Incorporation of ISR based sensor variable selection with RGA method*

Determining an optimum sensor variable set is still challenging even with the ISR based sensor ranking table like that shown in Table 2-3 because there are complex interactions between SVs and MVs in plasma etching. Therefore, interaction analysis between SVs and MVs is needed to make in order to enhance the performance of the ISR based sensor variable selection method.

The relative gain array (RGA) is a useful tool to analyze interactions between input and output variables in multiple input-multiple output (MIMO) control systems.^[40] One or more MVs can affect the interactions of CVs in a specific loop or all other control loops. Therefore, understanding the dependence of different MVs and CVs in the control scheme could be extremely helpful in designing and implementing a control scheme for a process.

If a control system with n controlled variables and n manipulated variables exists, the relative gain between a controlled and a manipulated variables is defined to be the dimensionless ratio of two steady-state gains:

$$\lambda_{i,j} = \frac{\left(\frac{\partial y_i}{\partial u_j}\right)_u}{\left(\frac{\partial y_i}{\partial u_j}\right)_s} = \frac{\text{open-loop gain}}{\text{closed-loop gain}} \quad (3-1).$$

For $i=1, 2, \dots, n$ and $j=1, 2, \dots, n$.

The RGA is defined as follows:

* The partial part of this chapter is taken from the author's publications.^[37-39]

$$\Lambda = \begin{matrix} & u_1 & u_2 & \cdots & u_n \\ \begin{matrix} y_1 \\ y_2 \\ \cdots \\ y_n \end{matrix} & \begin{bmatrix} \lambda_{11} & \lambda_{12} & \cdots & \lambda_{1n} \\ \lambda_{21} & \lambda_{22} & \cdots & \lambda_{2n} \\ \cdots & \cdots & \cdots & \cdots \\ \lambda_{n1} & \lambda_{n2} & \cdots & \lambda_{nn} \end{bmatrix} \end{matrix} \quad (3-2).$$

The RGA has some important properties and guidelines to understand and utilize it.^[41]

- (1) It is normalized because the sum of the elements in each row or column is equal to one.
- (2) The relative gains are dimensionless and thus not affected by choice of units or scaling of variables.
- (3) if $\lambda_{ij}=0$. The manipulated variable, u_j , will have no effect on the output controlled variable, y_i .
- (4) if $\lambda_{ij}=1$, the manipulated variable, u_j , affects the output, y_i , without any interaction from the other control loops in the system. From the definition of λ_{ij} , this implies that the gain loop with all loops open is equal to the gain loop with all other loops closed.
- (5) if $\lambda_{ij}<0$, the system will be unstable whenever u_j is paired with y_i , and the opposite response in the actual system may occur if other loops are opened in the system.
- (6) if $0<\lambda_{ij}<1$, other control loops ($u_j - y_i$) are interacting with the manipulated and controlled variable control loop.

According to the RGA properties, there are two rules to pair controlled and

manipulated variables. The first rule is to choose the RGA row element that is close to unity and the second rule is to avoid negative elements.

The RGA method has been extended to non-square systems.^[42] For a non-square system with more outputs than inputs ($m > n$), it is not possible to keep all outputs at their points. Therefore, the sense of perfect control in the definition of closed-loop gain should be modified. In this sense, a perfect control in the least-square sense is proposed. That is, a controller is designed in such a way that the steady-state offsets are minimized in the sense of least square. Then the non-square relative gain array (NRGA) is calculated as follows:

$$\Lambda^N = \mathbf{K} \otimes (\mathbf{K}^+)^T \quad (3-3).$$

The NRGA method has the similar properties to those of RGA method except that the sum of the elements in each row of the NRGA falls between zero and unity. It follows the same input-output pairing rules as those of the RGA, but due to the control in the least-square sense, the sum of squared errors (SSE) caused by uncontrolled SVs should be investigated.

The SSE for the entire system under perfect control of a selected square subsystem can be calculated as follows. If there is a $(m \times n)$ ($m > n$) non-square system with its transfer function matrix \mathbf{G} and n outputs for control are chosen, the system can be partitioned into

$$\begin{bmatrix} y_S \\ \text{---} \\ y_R \end{bmatrix} = \begin{bmatrix} \mathbf{G}_S \\ \text{---} \\ \mathbf{G}_R \end{bmatrix} \mathbf{u} \quad (3-4).$$

When considering steady-state error only, the input vector for the square subsystem in closed-loop is calculated by

$$\bar{\mathbf{u}} = \mathbf{G}_S^{-1} \bar{\mathbf{y}}_S^{\text{set}} \quad (3-5).$$

When the square sub-system is under perfect control, the steady-state error for all output is described by

$$\bar{\mathbf{e}} = (\mathbf{I}_{m \times n}^N - \mathbf{G}\mathbf{G}_S^{-1}) \bar{\mathbf{y}}_S^{\text{set}} \quad (3-6).$$

Thus for a particular choice of the square sub-system, \mathbf{G}_s , SSE is defined as

$$\text{SSE} = \sum_{i=1}^n \|\bar{\mathbf{e}}(i)\|_2^2 = \sum_{i=1}^n \left\| (\mathbf{I}_{m \times n}^N - \mathbf{G}\mathbf{G}_S^{-1}) \bar{\mathbf{y}}_{s,i}^{\text{set}} \right\|_2^2 \quad (3-7).$$

3.4. Recursive update algorithm for handling sensor data shift

As described in section 3.2.1, a huge number of sensors which have different physical properties and scales are employed in plasma etching. The data normalization of each sensor value can be another important issue for VM because according to the way of data normalization, the weight of certain sensor variables can be changed, which in turn might lead to wrong decision. Thus selection of data normalization is also crucial in plasma etching. In this chapter, mean centered and unit variance in Eq. (3-8) is chosen for data normalization.

$$X_{\text{normalization},i} = \frac{X_i - X_{\text{mean}}}{\sigma} \quad (3-8)$$

When the sensor data shifts like that shown in Fig. 3-1, VM model also should take care of those drift. Otherwise prediction performance by VM gets worse. There are two approaches to handling this issue.^[43] The first approach is to

maintain the data structure but only to update the coefficient for data normalization. The second approach is to frequently update the data structure by rebuilding the VM model with incoming new data sets. Updating the coefficients such as the mean and the standard deviation in our case would be more effective to handle the drift issue because the domain knowledge which is about the PM occurrence can be incorporated into the VM operation.

The mean and the standard deviation can be recursively calculated like that shown in the following Eqs. (3-9) and (3-10).

$$\bar{x}_n = \frac{n-1}{n} \bar{x}_{n-1} + \frac{1}{n} x_n \quad (3-9)$$

$$\sigma_n^2 = \left(\frac{1}{n-1} \right)^2 \sum_{i=1}^n (x_i - \bar{x}_n)^2 = \left(\frac{1}{n-1} \right)^2 \left[\left(\sum_{i=1}^n x_i^2 \right) - n \left(\sum_{i=1}^n x_i \right)^2 \right] \quad (3-10)$$

With the above equations, the coefficients of data normalization will be updated, based on the domain knowledge.

3.5. Results and discussion

3.5.1. Optimum sensor variable selection for VM

Since the process result like CD are closely related to plasma SVs and the plasma SVs are manipulated by MVs, selecting plasma SVs corresponding to MVs is a proper approach to determining an optimum input variable set for VM. Specifically, selecting at least one SV per MV is desirable for controller robustness.

In order to determine the upper mentioned optimum input variable sets for VM, a

systematic variable selection which is the integration of the ISR-based sensor variable selection in section 2.3 with the RGA method in section 3.3 is suggested. As a first step, MVs that are effective to control CD are determined based on engineers' knowledge. Then top ranked plasma sensor variables for each MV are chosen, which can be obtained from the ISR based sensor ranking table. The number of top sensor variables per MV is determined, considering the total number of the selected MVs. Then sensor variables with zero steady-state gain elements for several MVs are excluded because the SV with zero gain for a MV implies that it does not respond to the particular MV. After that, NRGAs of the steady-state gain matrix between MVs and SVs is calculated. Table 3-1 summarizes the NRGAs of (18 x 7) steady-state gain matrix, where the relative gains of each MV which are close to unity as much as possible are in bold.

According to the pairing rules from the RGA in section 3.3, possible MV-SV pairings can be determined as follows: (Pressure – OES10 or OES 8), (Source Power – OES 11 or OES 1), (Bias Power – Not Available), (Gas 1 Flow – OES 11), (Gas 2 Flow – Collision Rate or OES 4), (Gas 3 Flow – 4th Harmonics), and (Gas 4 Flow – Electron Density).

These selected possible pairings by the RGA rules are not always valid for non-square systems,^[42] so the SSE caused by uncontrolled SVs should be investigated for all possible (7 x 7) square sub-systems. Table 3-2 summarizes the top ten square sub-systems having lowest SSEs, which is calculated by the Eq. 3-7. The top square sub-system consists of collision rate, OES 8, electron density, OES 1, OES 4, 2nd harmonics, and 4th harmonics. These selected SVs are a part of the selected nine SVs through the RGA rules above. The other square sub-systems in Table 3-2

also include at least six SVs matching the selected SVs through the RGA rules. This suggested that the selected SVs through the RGA rules are also valid for the non-square system.

Table 3-1. The calculated NRGAs of the (18 x 7) steady-state gain matrix

	Pressure	Source Power	Bias Power	Gas 1 Flow	Gas 2 Flow	Gas 3 Flow	Gas 4 Flow
Collision Rate	0.000	-0.019	0.138	0.560	0.651	-0.284	-0.047
OES14	0.588	-0.362	0.000	-0.435	0.314	0.108	-0.074
OES10	0.624	-0.381	0.000	-0.513	0.406	0.142	-0.122
OES 9	0.402	-0.273	0.000	-0.388	0.333	0.102	-0.043
OES 13	-0.235	0.185	0.000	0.229	-0.129	-0.054	0.105
OES 11	-0.884	0.783	0.000	0.982	-0.702	-0.194	0.311
OES 12	0.466	-0.310	0.000	-0.420	0.388	0.143	-0.119
OES 15	0.037	-0.046	0.000	-0.053	0.120	0.029	0.027
OES 16	-0.021	0.031	0.000	0.033	-0.004	-0.009	0.047
OES 8	0.755	-0.469	0.000	-0.659	0.509	0.149	-0.094
Electron Density	0.000	0.180	0.349	0.000	-0.670	0.162	0.972
OES 17	0.157	-0.055	0.000	-0.047	0.023	0.032	-0.040
OES 1	-1.289	1.358	0.000	1.455	-1.103	-0.283	0.433
OES 4	-0.198	0.446	-0.013	-0.222	0.593	-0.156	0.014
2 nd Harmonics	0.000	-0.077	0.338	0.329	0.106	0.493	-0.202
OES 2	0.236	0.087	0.000	-0.020	0.165	-0.046	-0.067
4 th Harmonics	0.000	0.020	0.185	0.169	0.000	0.625	0.000
OES 18	0.362	-0.100	0.003	0.000	0.000	0.042	-0.102

Note: The relative gains of each MV close to unit as much as possible are in bold.

Table 3-2. The top 10 square sub-systems having lowest SSEs

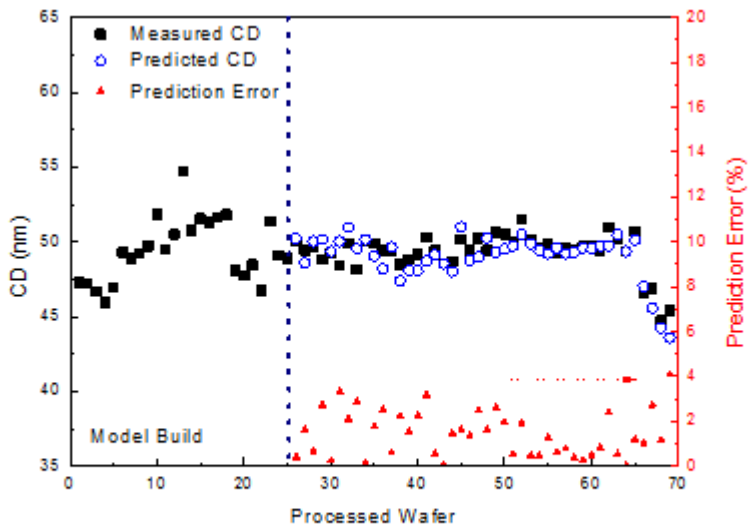
Square Sub-system	1	2	3	4	5	6	7	8	9	10
	C/R									
	OES 8	OES 8	OES10	OES12	OES11	OES14	OES10	OES 9	OES12	OES 9
	E/D	E/D	E/D	E/D	OES 8	E/D	E/D	E/D	E/D	E/D
Selected SVs	OES 1	OES 1	OES 1	OES 1	E/D	OES 1				
	OES 4	2 nd Ha	OES 4	OES 4	OES 4	OES 4	2 nd Ha	OES 4	2 nd Ha	2 nd Ha
	2 nd Ha	OES 2	2 nd Ha	2 nd Ha	2 nd Ha	2 nd Ha	OES 2	2 nd Ha	OES 2	OES 2
	4 th Ha									
SSE	9.975	10.142	10.166	10.304	10.308	10.313	10.330	10.350	10.367	10.445

Note: C/R: Collision Rate, E/D: Electron Density, 2nd Ha: 2nd Harmonics, 4th Ha: 4th Harmonics

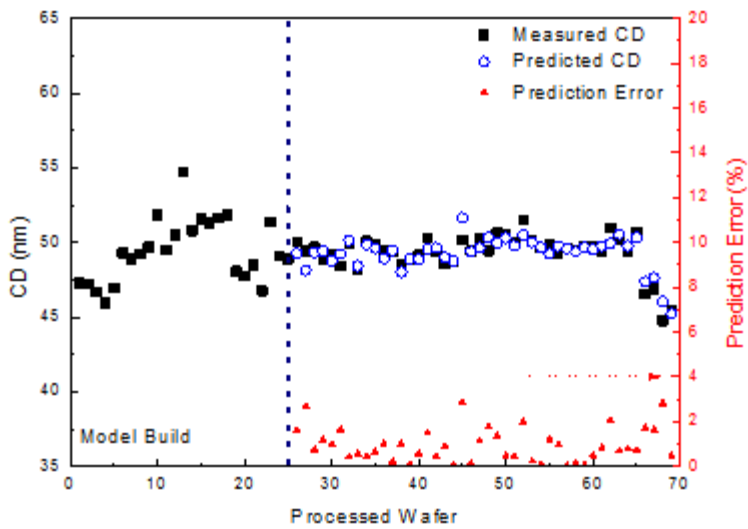
3.5.2. Reliable VM system by simple linear regression methods

With the top square sub-system selected in section 3.5.1, VM models to predict a metal line CD in a DRAM device is built by applying the linear regression methods like multiple linear regression (MLR) and partial least squares regression (PLSR). Since an optimum input variable set which reflects physical properties of plasma is selected, it is believed that a robust VM model without employing more complex regression methods such as neural network^[44] and support vector regression (SVR)^[45] could be built.

Figure 3-2 shows the performance of the VM system built with MLR and PLSR methods. 25 wafers are prepared for VM model construction, some of which have a CD value larger than the normal specification and the other 40 wafers under normal operations are utilized for the performance check of the VM systems. The prediction error of both models is less than 5% if several outliers which come from previous process steps are excluded. The mean absolute percentage error (MAPE) of the VM system is larger than other published VM results^[31, 38] but considering that the VM system in this thesis predicts much more complicated CD than etch rate or etched depth in those papers and furthermore the number of input variables employed in the VM model is relatively small, the ISR based sensor variable selection introduced in this thesis is useful. In addition, it might be the first one to implement the robust CD VM with less than 10 input variables in plasma etching.



(a)



(b)

Figure 3-2. Metal line CD prediction performance of VM systems: (a) MLR and (b) PLSR are applied to build the VM model.

3.5.3. Recursive coefficient update to handle sensor data shift

As is described in section 3.2.2, a performance of a VM system in plasma etching might be worse after wet cleaning unless the model of VM covers the plasma sensor data shift. Figure 3-3 shows the CD prediction performance of the VM system across wet-cleaning. After wet cleaning, the prediction error of the VM system jumps from less than 3% before wet cleaning to higher than 7%. This situation happens after almost every wet cleaning, which implies that the lifetime of the VM system ends once wet cleaning starts.

In order to extend the lifetime of the VM system, the model of the VM system should be updated. A simple way to update the model of the VM system is to rebuild a new model of the VM system with the new training sets after wet cleaning. Re-building the whole model of the VM system, however, is not a good approach in semiconductor manufacturing because it sacrifices additional production wafers and the wafer-to-wafer quality control with the VM system is suspended during the period of the modeling rebuild.

There have been several studies on recursive update of PLS.^[46-48] Those recursive update algorithms are based on historical data and then wait for accumulation of new data points to converge. Since recursive modeling still uses all the input and output data points from the beginning which can lead to computational issues, they are not proper for the case of only input variables' shift in plasma etching. Thus the recursive coefficient update technique in data normalization described in section 3.4 is more cost-effective and more appropriate in the sensor data shift after wet

cleaning.

Figure 3-4 shows the results in which the recursive coefficient update in data normalization is applied to input variables. By applying the technique after wet cleaning, the prediction error is significantly reduced to less than 5%, which is close to that of the VM before wet cleaning. There is an initial drift of the prediction error at the beginning of the first several wafers after wet cleaning. This initial drift can be handled by applying different weighting of the several first wafers when the mean and standard deviation are recursively calculated. This technique is successively applied to both MLR and PLSR based VM systems and it is believed that the technique can be applied to other regression techniques in which initial data normalization is required.

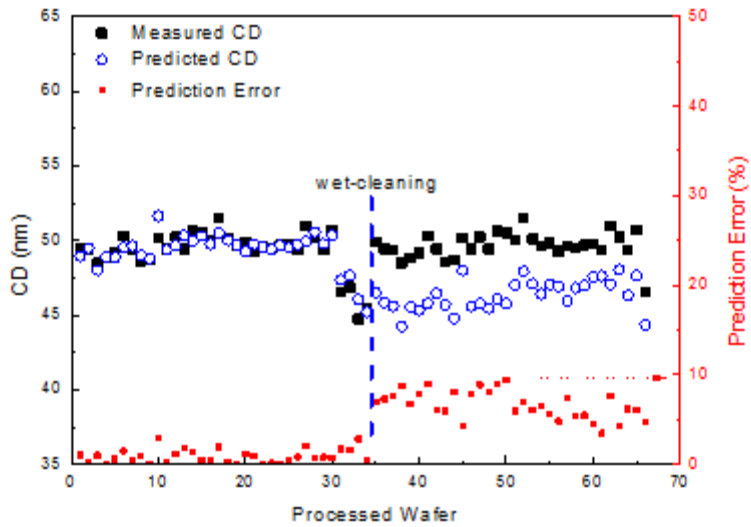


Figure 3-3. Metal line CD prediction performance of PLS based VM systems without the recursive coefficient update technique.

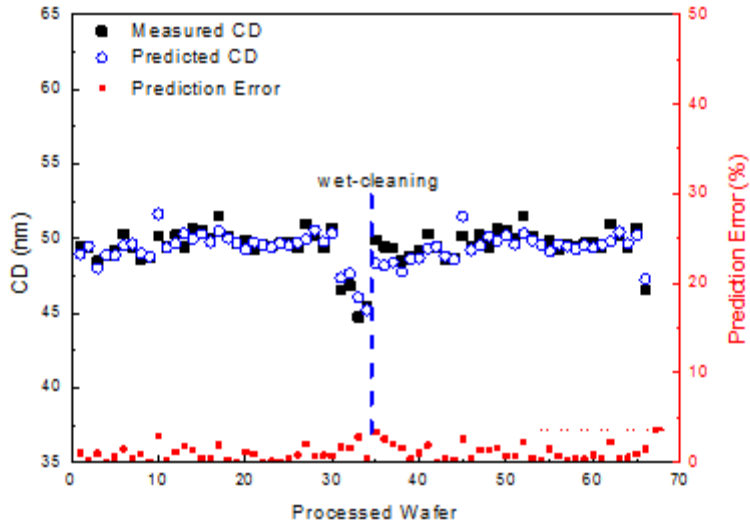


Figure 3-4. Metal line CD prediction performance of PLS based VM system with the recursive coefficient update technique.

3.6. Conclusions

Issues in implementing a robust VM for plasma etching are discussed in this chapter: state-of-the art plasma sensors which are more responsive to process results than hardware gauges to measure equipment states, effective selection of plasma sensor variables responding to individual MV, sensor data shift across PM which is caused by dynamics in semiconductor manufacturing. In order to handle selection of plasma sensor variables, ISR based sensor selection is employed, which can be a starting point for variable selection of VM. The initial variable set based on ISR can be refined by the interaction analysis from NRGGA which can reduce the number of input variables for VM. With the help of plasma sensor variables and its optimum sensor variable selection, simple linear regression methods such as MLR and PLSR are successfully applied to predict a metal line CD in plasma etching. The MAPE of the VM systems is less than 5% even in the case of complicated CD prediction. Sensor variable shift effects across wet cleaning which hurts a reliability of the VM system in plasma etching is reduced to level of MAPE before wet cleaning with a cost-effective recursive coefficient update technique.

CHAPTER 4 : Chamber Conditioning after Wet Cleaning

4.1. Introduction

As chamber conditions gradually change with wafer processing, PM such as wet cleaning is an inevitable and periodic event in semiconductor manufacturing. Because wet cleaning, one of the most frequent PMs in semiconductor manufacturing, initializes chamber conditions, a chamber conditioning process called chamber seasoning follows the wet cleaning until the chamber conditions return to normal for production. Specifically, in plasma etching where performance is significantly affected by chamber surface conditions,^[49-55] chamber seasoning is an indispensable process after the wet cleaning.

The practice in chamber seasoning for plasma processes is to run the same recipe as the production process by using non-pattern wafers (NPWs). In plasma etching, however, this practice is not frequently applicable because etch by-products to be deposited on the chamber wall can differ according to the wafers processed. Thus, most plasma etching tools have a significant process drift for a certain period after wet cleaning. The solution of this problem is conceptually simple; making etch by-products the same as those for production so that the chamber wall can be deposited by the same composition of etch by-products.

This chapter introduces a systematic approach to generating chamber seasoning recipes, which enables imitating etch by-product environments from production wafers even with NPWs. The approach of this chapter is to utilize OES in order to

find critical etch by-products for chamber seasoning. A dynamic optimization technique employed in a MIMO control system is applied to find an optimum condition, which is based on the signal from the OES. For this purpose, a newly developed signal processing technique for OES is introduced, which enables a quantitative analysis of OES spectra. The developed systematic methodology was applied to an inductively coupled plasma reactor that was suffering from a serious process drift after wet cleaning. Its effectiveness was demonstrated in a manufacturing environment for a DRAM device. Hopefully, the systematic approach introduced in this chapter will be disseminated to semiconductor manufacturers who experience serious process drifts after wet cleaning.

4.2. Experiment

The plasma etch system used in this chapter is an inductively coupled plasma reactor from Applied Materials, Inc. In this system, a shallow trench etch process for a DRAM device is performed, which suffers from a serious process drift after wet cleaning. The OES is utilized for characterizing plasma emission under various chamber conditions. Sharp peaks of OES spectrum which come from atomic emission of radicals in the plasma[22] are used to determine the signature of the required chamber condition. The raw OES spectrum is pre-processed to be utilized as a reference for plasma control. This is enabled by the self-background normalization technique.^[56]

The dynamic optimization technique for a MIMO control strategy is applied to find an optimum chamber seasoning recipe under inherently non-linear plasma environments. Based on physical analysis and engineering experience, MVs of recipe are determined. Those MVs are connected with selected OES peaks as CVs, which is enabled by the design of experiments (DOE) based model. Important OES peaks responsible for chamber seasoning are automatically selected by the comparison of the self-background normalized OES spectra between production wafers and NPWs. The effectiveness of the optimized recipe is evaluated in terms of OES spectra and the etch rate of Si in a manufacturing environment for a DRAM device.

4.3. Issues in wet cleaning for plasma etch systems

4.3.1. Serious process drift after wet cleaning

Figure 4-1 shows an etch rate trend after wet cleaning in a Si trench etch process for a DRAM device. As is shown in Fig. 4-1, the etch rate of Si in the plasma etch system drifts until about 60 hours of RF on time. This explains why the etched depth of the Si trench in this system dropped more than 5% right after wet cleaning and gradually stabilized over time. This behavior of the etch rate drift over time is repeating for every wet cleaning, which is a common problem that semiconductor manufacturers face.

Since wet cleaning initializes chamber conditions, a chamber seasoning should follow until the chamber conditions get back to normal for production. In practice, chamber seasoning for plasma processes run the same recipe as the production process by using NPWs. In plasma etching, however, this practice not frequently applicable because etch by-products to be deposited on the chamber wall differ according to the wafers processed, which is clearly detected in OES like that shown in Fig. 4-2. This difference in plasma characteristics makes the chamber condition different from what it should be. As a result, most of the plasma etching systems have significant process drifts for a certain period after wet cleaning.^[16, 52, 55] Thus, the recipe of chamber seasoning should be optimized in such a way that the plasma characteristics (or at least the etch by-products) can be matched with those from the target production process.

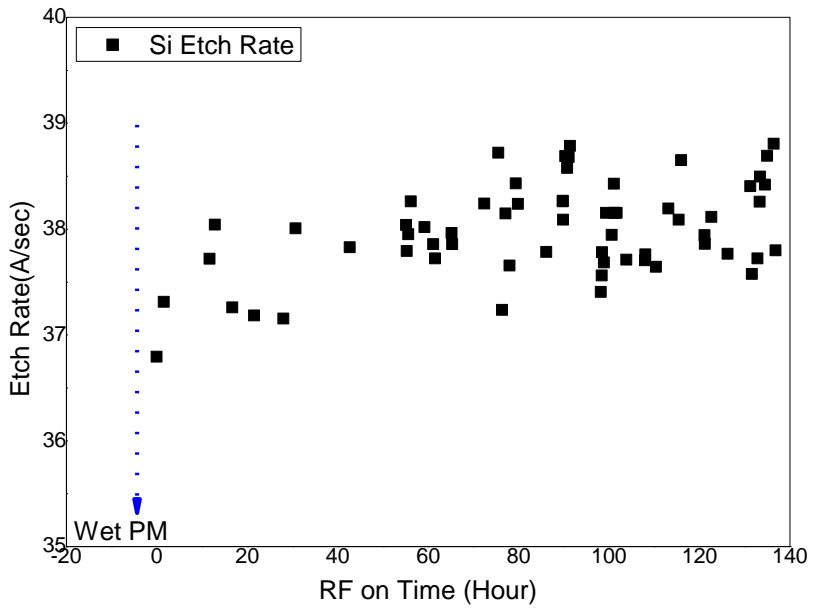


Figure 4-1. Si etch rate trend after wet cleaning.

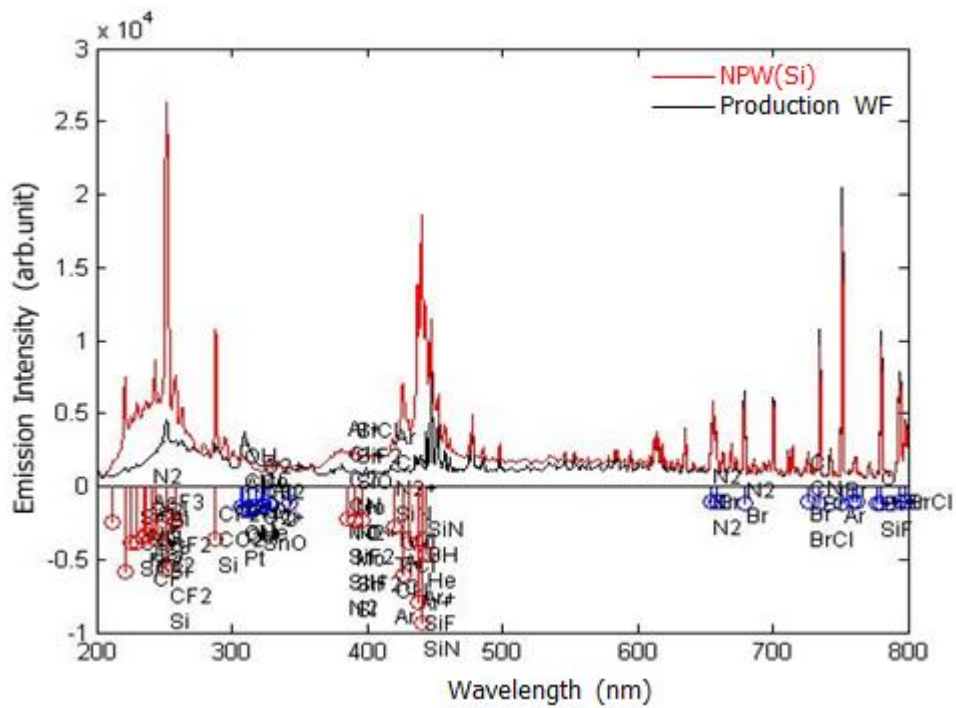


Figure 4-2. OES spectra over different wafers (non-pattern Si wafer and production wafer) with the same plasma condition.

4.3.2. OES data drift between and across preventive maintenance

The utilization of OES has been limited to the endpoint detection in plasma etching because the OES signal contains the nonlinear attenuation from the optical paths such as an optic window, fiber optic cable, and optical connectors. Among those attenuation sources in OES, the optical window facing the plasma directly is always influenced by the deposition of etch by-products. This phenomenon is called as window clouding effect and it adds complexity in analyzing the plasma emission spectra. Figure 4-3 shows the changes in spectra for different RF on times. The intensity of each wavelength decreases from one PM to the next PM, and the PM always accompanies the wet cleaning that cleans or replaces the clouded optical window. The magnitude of intensity drop is all different in each wavelength as indicated in the arrows of the figure.

In order to utilize the OES spectra as a reference of plasma control, a novel signal processing technique, self-background normalization is developed.^[56] This pre-processing technique enables compensating for the window clouding effect and other noise factors in OES that complicate a numerical analysis of the plasma spectrum. The idea assumes the two spectral modes in plasma emission, an atomic emission mode of sharp peaks and a molecular emission mode of gentle slope. As shown in Fig. 4-4, the valley points in the spectrum are connected with quadratic interpolation. Thus, all data points can be normalized with the baseline, which comprises the molecular modes and the subsidiary difference from the attenuation sources.

The optical intensity measured by OES is a product of wavelength λ and transmittance T, as shown in Eq. 4-1. The total transmittance is a product of the transmittance values of all the components in the optical paths: Eq. 4-2.

$$I_{OES}(\lambda) = I_{plasma}(\lambda) \times T_{total}(\lambda) \quad (4-1)$$

$$T_{total}(\lambda) = T_{window}(\lambda) \times T_{fiber}(\lambda) \times T_{connectors}(\lambda) \quad (4-2)$$

The transmittance of adjacent wavelength is almost identical because the transmittance curves are continuous in wavelength domain.^[57] Thus, the transmittance of a peak wavelength can be estimated to lie between the transmittance of adjacent valleys. This transmittance term can be eliminated by dividing the peak intensity by the estimated background intensity of the peak wavelength, which is shown in Fig. 4-5. This normalization process is one of the results that enable quantitative comparison of the plasma spectra which are affected by the chamber environments.

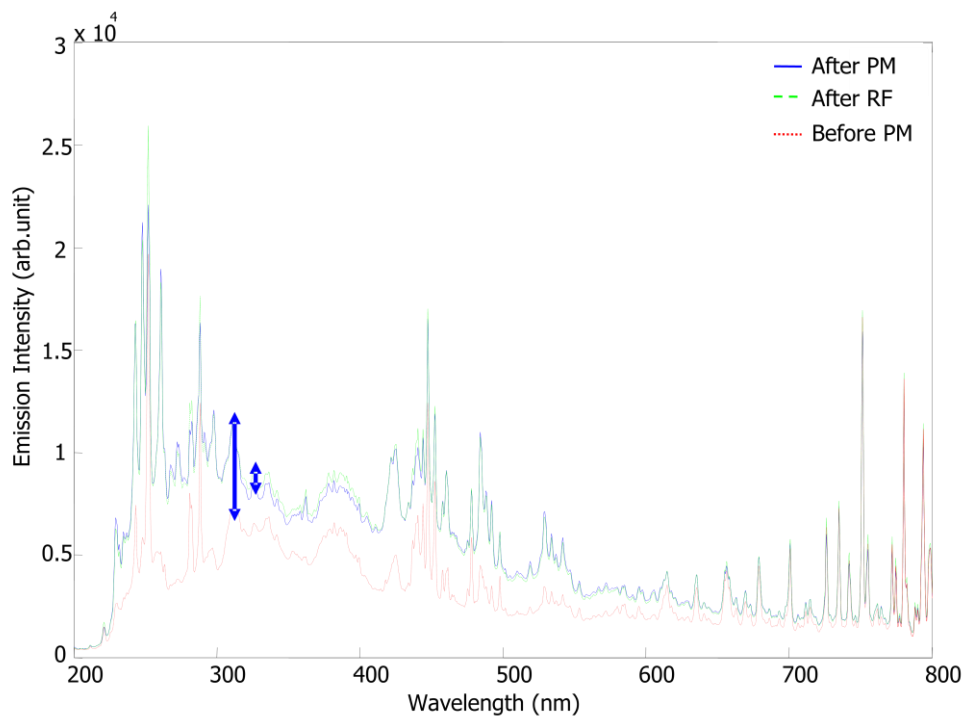


Figure 4-3. Spectral changes with time during a PM period.

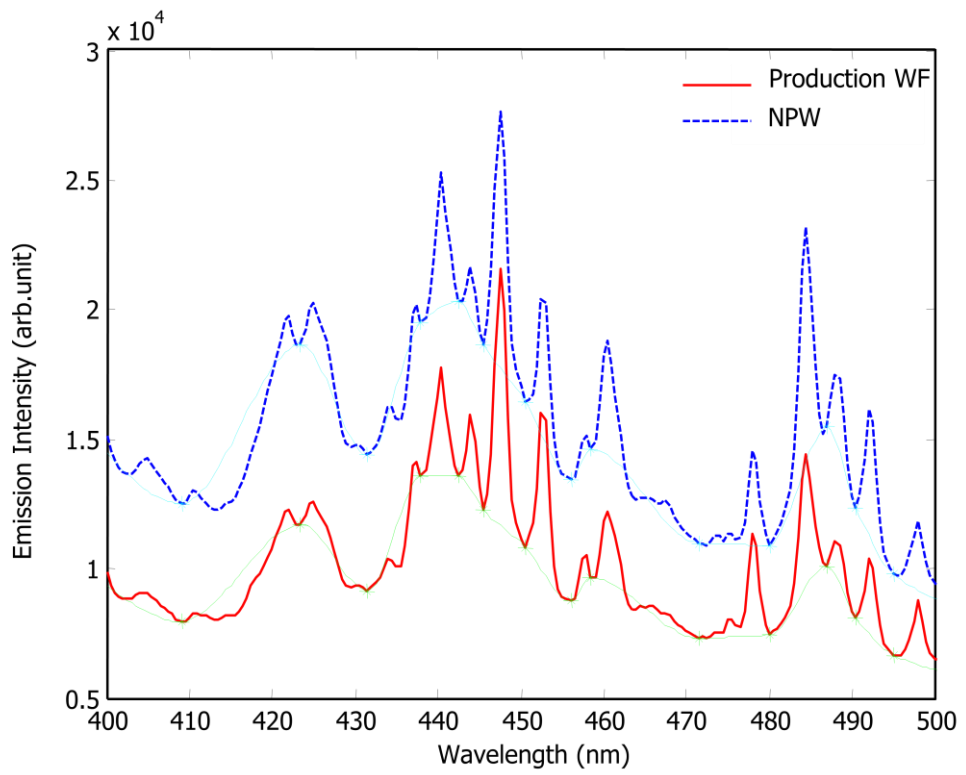


Figure 4-4. Raw spectra of different wafers with the same recipe.

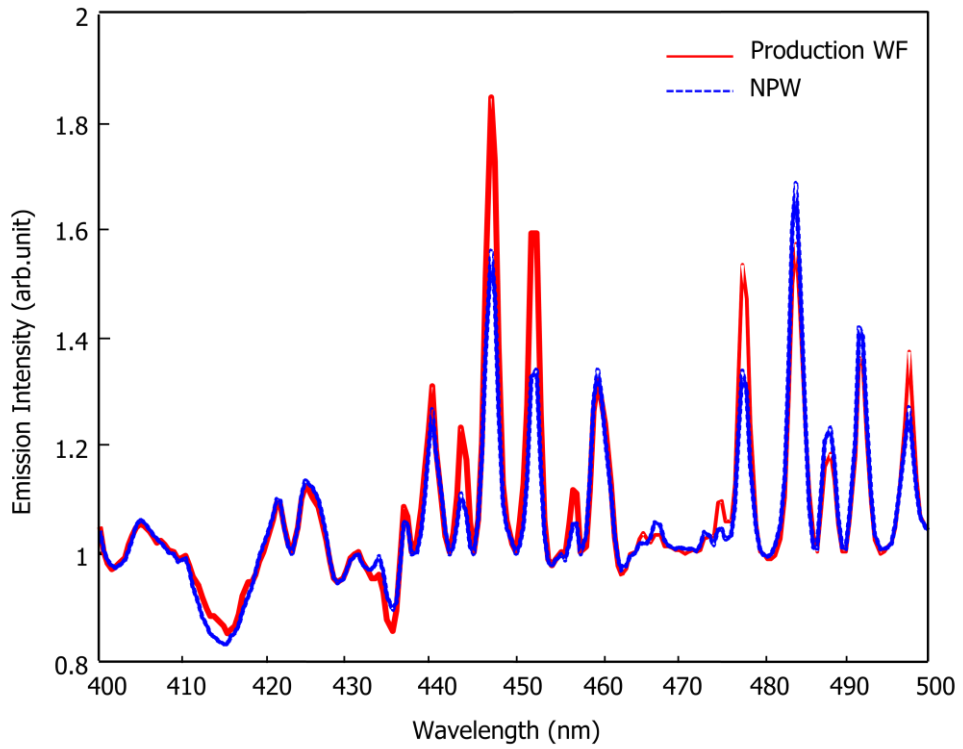


Figure 4-5. Normalized spectra of a production wafer and NPW showing the big different wavelength positions in terms of intensity.

4.3.3. Optimization problems with OES data

In order to achieve optimum recipe conditions for chamber seasoning with OES data, selection of the important OES peak as a CV in a plasma control model should be done effectively. Selection of the important OES peak is made by comparing the normalized OES spectrum from NPWs and production wafers. Figure 4-6 shows a result comparing normalized OES spectra from different wafers. The step chart below the x axis identifies the wavelengths of relatively larger difference between the wafers and the species related to the wavelengths. The length of each stem stands for the difference of the normalized peak intensity between the wafers. For instance, the blue step of length 2 means the normalized intensity of the blue spectrum (production wafer) is 200% higher than the NPW. The length of the step becomes a control target to be manipulated by MVs, which leads to matching plasma environment.

The selection of proper MVs is another challenge in designing a control system. Since the number of MVs determines the number of experiments in design of experiments (DOE), it is desirable to reduce the number of MVs as much as possible. Since OES essentially measures plasma chemistry, recipe parameters related to plasma characteristics such as gas flow rate, source power and/or pressure are chosen as MVs.

The empirical model which is composed of the normalized OES intensity and MVs is built by the Box-Behnken design. This model requires the smallest number of experiments among the quadratic models. Figure 4-7 shows an empirical model space of Box-Behnken design where 3 MVs are included. The 15 experiments of 13 different plasma conditions are required for this design because the base

condition (origin) is repeated three times. The results of these experiments can induce a full quadratic model, where y is the normalized peak intensity of the wavelength chosen for CV and x is the recipe parameters chosen for MV.

The quadratic model equation with higher order and interaction terms relating MVs and CVs can be defined as follows:

$$y_i = f_i(u_1, u_2, u_3) + offset_i \quad (4-3)$$

After Eq. 4-3 is obtained, an optimization problem with constraints can be solved with a quadratic objective function described in Eq. 4-4 in order to obtain optimum MVs in MIMO control.^[58-61]

$$J = \min_{u_1 \dots u_9} \sum_{i=1}^l w_i (y_{i,t} - y_i)^2 \quad (4-4)$$

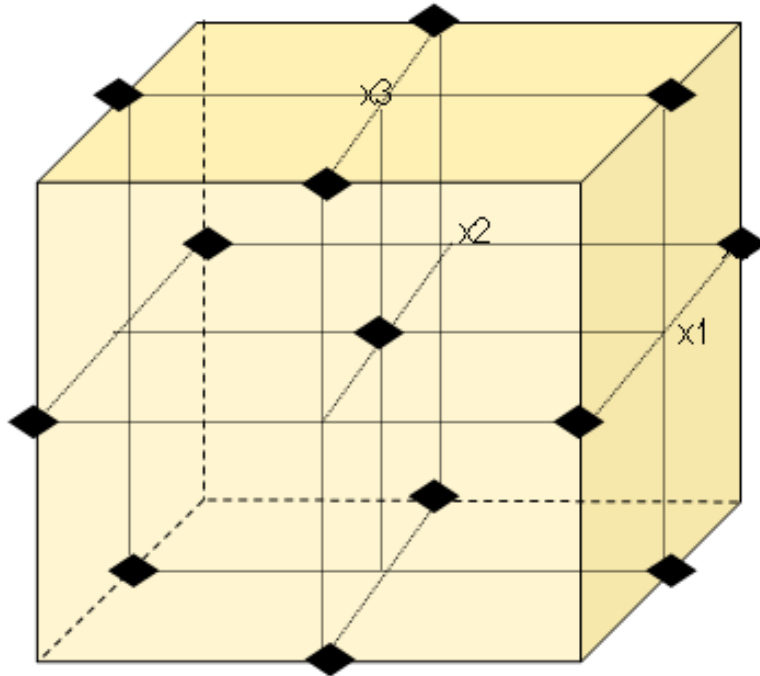


Figure 4-7. Empirical model space of 3 factor Box-Behnken design.

4.4. Systematic optimization of chamber seasoning conditions

4.4.1. Step-by-step procedure to optimize chamber seasoning conditions through OES

Figure 4-8 illustrates a process flow for optimization of a chamber seasoning condition. The first step is to collect OES spectra from production wafers and NPWs. The second step is to compare the normalized OES spectra by the technique described in section 4.3.2 and to determine important OES peaks, based on the difference of the two spectra. The third step is to select MVs based on the recipe condition and plasma knowledge. Gas flow rates and source power or pressure are selected as MVs for the Si trench etch case. The next step is to run a set of experiments to build a model between the selected OES peaks and MVs. The test conditions for each step are summarized in Table 4-1. Based on the Box-Behnken design with three factors, 15 experiments which include 5 etch steps are made over NPWs.

With the model built by the Box-Behnken design, optimization problems of the Eq. 4-4 are solved by using the *fmincon* function in MATLAB™. Then the solution of the optimization problem becomes a new recipe condition for chamber seasoning. Finally the OES spectrum applied by the new recipe condition over NPWs is compared with the spectrum over production wafers. If the comparison is acceptable to the pre-determined specification, then the recipe is applied to the chamber seasoning condition. If not, the DOE and optimization steps are repeated.

Table 4-1. Experimental design for the Box-Behnken design for an OES to MVs model.

No	1 st Step			2 nd Step			3 rd Step			4 th Step			5 th Step		
	N ₂	CF ₄	Pres	Cl ₂	Br	Pres	O ₂	PWR	Pres	N ₂	CF ₄	Pres	Cl ₂	Br	Press
1	5	100	10	140	120	30	100	700	15	5	100	10	120	120	8
2	10	60	40	140	160	60	130	1000	15	10	60	40	120	140	12
3	5	60	25	140	140	45	115	850	15	5	60	25	160	160	8
4	0	60	10	120	140	30	100	1000	15	0	60	10	140	160	12
5	0	20	25	140	140	45	130	850	25	0	20	25	160	140	4
6	5	60	25	120	120	45	115	1000	25	5	60	25	140	120	4
7	5	20	10	120	140	60	130	700	15	5	20	10	140	160	4
8	5	100	40	160	160	45	115	700	25	5	100	40	140	140	8
9	0	60	40	140	140	45	115	850	15	0	60	40	120	160	8
10	5	60	25	120	160	45	115	1000	5	5	60	25	140	140	8
11	10	100	25	160	140	60	115	700	5	10	100	25	160	120	8
12	10	60	10	140	120	60	100	850	25	10	60	10	160	140	12
13	10	20	25	160	120	45	130	850	5	10	20	25	140	140	8
14	5	20	40	140	160	30	100	850	5	5	20	40	120	140	4
15	0	100	25	160	140	30	115	850	15	0	100	25	140	120	12

Note: Pres means pressure and PWR stands for source power.

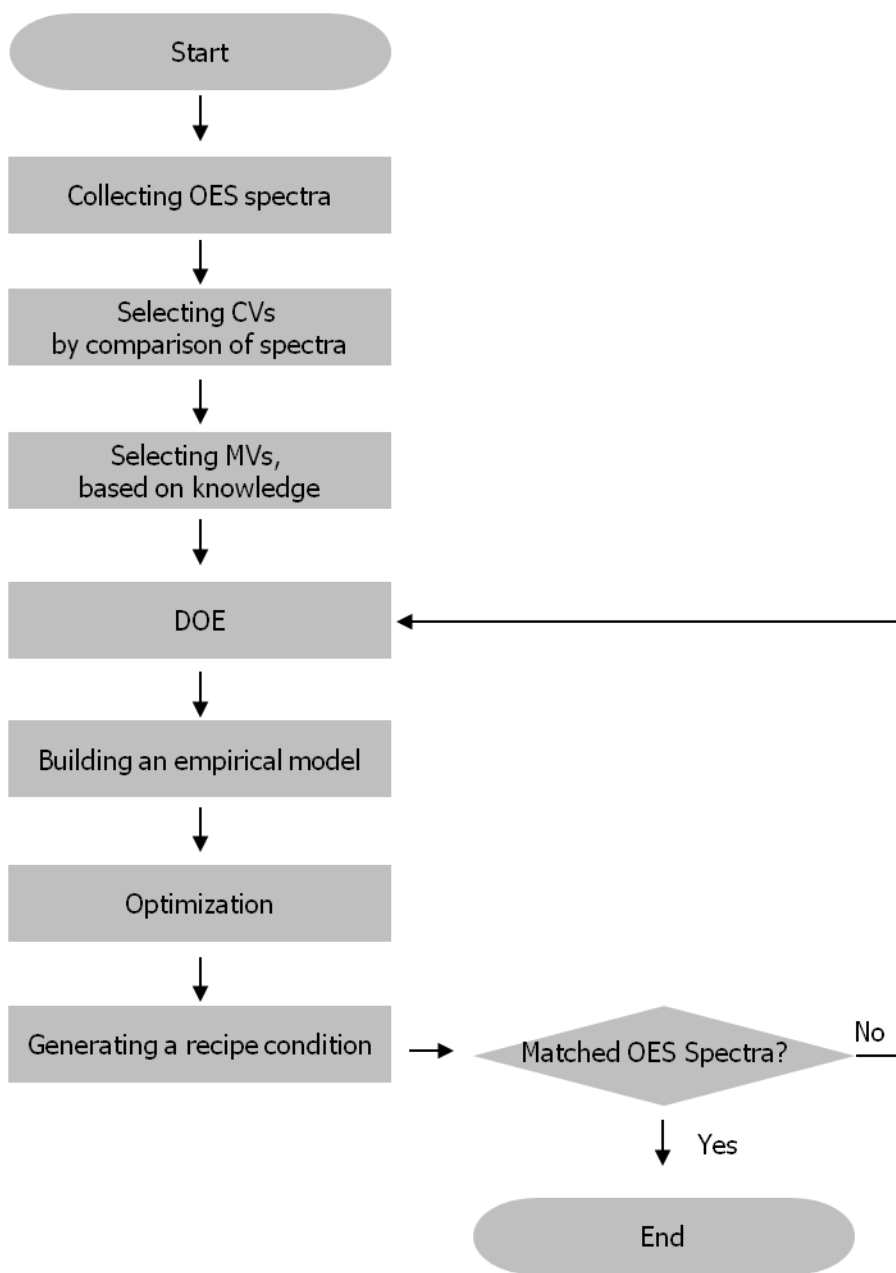


Figure 4-8. A process flow for optimization of a chamber seasoning condition.

4.4.2. Application of step-by-step procedure to Si trench etch process

Table 4-2 summarizes how the optimum plasma condition is changed as a result of the step-by-step procedure described in section 4.4.1. The values of gas flow rates and pressure in the proposed recipe are distinguished from those of the original recipe normally used for chamber seasoning so far. These MV values are not readily considered by engineers. For instance, the magnitude of CF₄ flow rate change in 1st and 4th steps is higher than expected.

Prior to using the optimized seasoning condition, the spectra of the original seasoning recipe and the optimized recipe over NPWs are compared with those of the production process. As is shown in Fig. 4-9, the difference between the production process and the optimized seasoning condition is dramatically decreased especially in terms of CVs when compared with the original seasoning condition. This means the suggested seasoning recipe succeeds in imitating the production plasma environment over different NPWs.

The optimized seasoning recipe is applied to a plasma reactor suffering from severe etch rate drift after wet cleaning, which is shown in Fig. 4-1. The results are summarized in Table 4-3. In terms of Si etch rate, the value is perfectly matched to the value before wet cleaning. In addition, the drift of Si trench depth completely disappears, which is not shown in this thesis.

Table 4-2. Suggested MV settings from the optimization problems.

	1 st Step	2 nd Step	3 rd Step	4 th Step	5 th Step
MV1	0 → 7	150 → 162	100 → 101	0 → 0	150 → 174
	N ₂ (sccm)	Cl ₂ (sccm)	O ₂ (sccm)	N ₂ (sccm)	Cl ₂ (sccm)
MV2	40 → 108	150 → 174	1000 → 924	40 → 73.0	150 → 137
	CF ₄ (sccm)	Br (sccm)	Source Power (W)	CF ₄ (sccm)	Br (sccm)
MV3	40 → 43	50 → 65	10 → 4.5	40 → 26.5	10 → 4.0
Pressure (mT)					

Table 4-3. Comparison of Si etch rate according to different plasma conditions.

	Original Seasoning (Right after Wet Cleaning)	Optimized Seasoning (Right after Wet Cleaning)	Production Plasma
Si Etch Rate (A/sec)	36.8	38.0	37.8

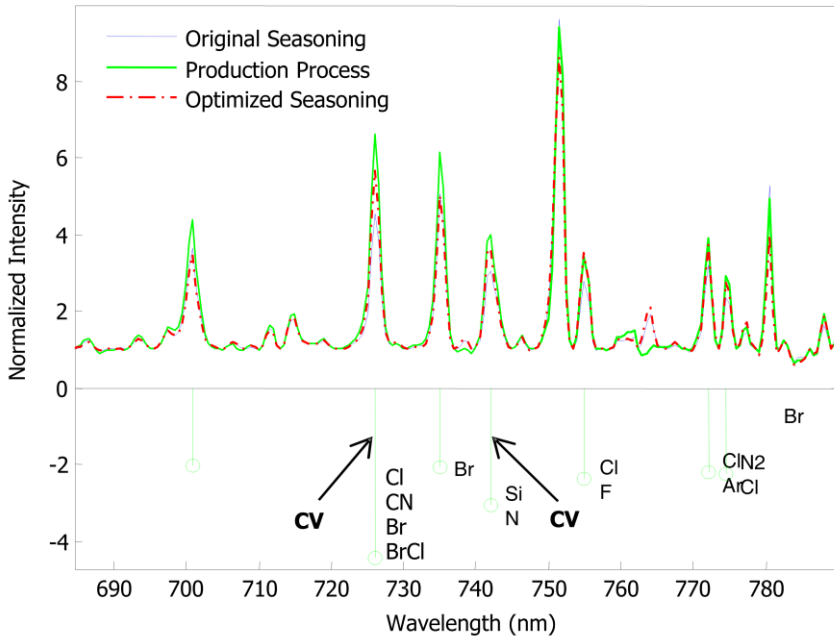


Figure 4-9. Comparison of the normalized spectra around CV in each plasma.

4.5. Conclusions

A systematic procedure to optimize chamber seasoning conditions with OES was suggested to address the process drift after wet cleaning in plasma etching. In order to achieve a quantitative analysis of plasma spectra without being disturbed by noises from optic systems, a self-background normalization technique is introduced. Also in order to automatically determine optimum seasoning conditions, a MIMO control strategy is applied and the optimum condition is obtained by solving the quadratic optimization problems. The suggested methodology is demonstrated in a DRAM manufacturing environment suffering from a serious process drift after wet cleaning. Hopefully, the proposed methodology in this chapter can be adapted to semiconductor manufacturers experiencing similar issues right after wet cleaning.

CHAPTER 5 : Chamber to Chamber Matching by MIMO Controller Design

5.1. Introduction

The semiconductor manufacturing is a capital-intensive industry, in which the cost of building a new fab is estimated to be over several billion U.S. dollars. Advances in semiconductor device technologies typically require additional investments to upgrade manufacturing equipment. The rapid shrinkage of the semiconductor device drives manufacturing equipment to be equipped with more precise capabilities so that equipment can meet process performance targets under a tight process window. In addition, the number of chambers employed in a process can be larger than 30 in one fab, and those chambers can have considerable performance deviation in some cases even though they are expected to have the same model. Thus, costs of fab operation are growing and techniques to maintain equipment and process within a desired specification are critical.

The semiconductor manufacturing includes more than 300 sequenced processing steps, which can fall into four major categories such as patterning, deposition, diffusion, and removal. Since each processing step operates multiple chambers to maximize productivity, it is crucial to ensure that each chamber running the same process step yields the same process results. Given that one chamber generally consists of several thousands of parts and tens of part-kits are changed during every PM, it has been a challenge for semiconductor manufacturers to keep performance of multiple chambers the same.

This chapter introduces a systematic technique using a decomposed etch rate map to match multiple chamber performance in semiconductor manufacturing. Among semiconductor manufacturing processes, plasma etching is chosen for the study because the inherent complexity of plasma makes it difficult to match chamber performance.^[62, 63] To effectively match chamber performance, an equipment control methodology is applied to plasma etching, which includes optimum variable selection, controller design, and dynamic optimization techniques. For example, optimum MVs are identified through SVA and RGA methods. Then, a recipe controller is designed with the optimum MV sets tied with particular CVs. Each recipe controller finds optimum MV settings with a constrained dynamic optimization technique and its MV settings are applied for each chamber to match performance. It is believed that the step-by-step approach introduced in this chapter will help semiconductor manufacturers effectively handle their chamber matching issues.

5.2. Experiment

A commercial capacitively coupled plasma (CCP) reactor for a 300mm wafer shown in Fig. 5-1 is employed in this chapter. The source is powered by the 162 MHz generator, and the bias is powered by both 13.56 and 2 MHz generators. The chamber has a narrow gap of 32mm and a volume of 42l. The pressure can be adjusted under 10mT by using the turbo molecular pump with 3000 l/s capacity. To adjust the symmetric uniformity in the performance, a split type baffle and a temperature tunable electrostatic chuck (ESC) are employed. To achieve uniform plasma characteristics, charged species tuning unit (CSTU) and neutral species tuning unit (NSTU) are applied, which can control the ion and the neutral flux.[64] The operating conditions are as follows: pressure was controlled from 9 to 11 mT. Source and bias powers were changed within 5% range. The etch gases are mixture of C₄F₆, Ar, and O₂. CSTU and NSTU were changed from 2 to 4 according to their sensitivity to plasma characteristics.

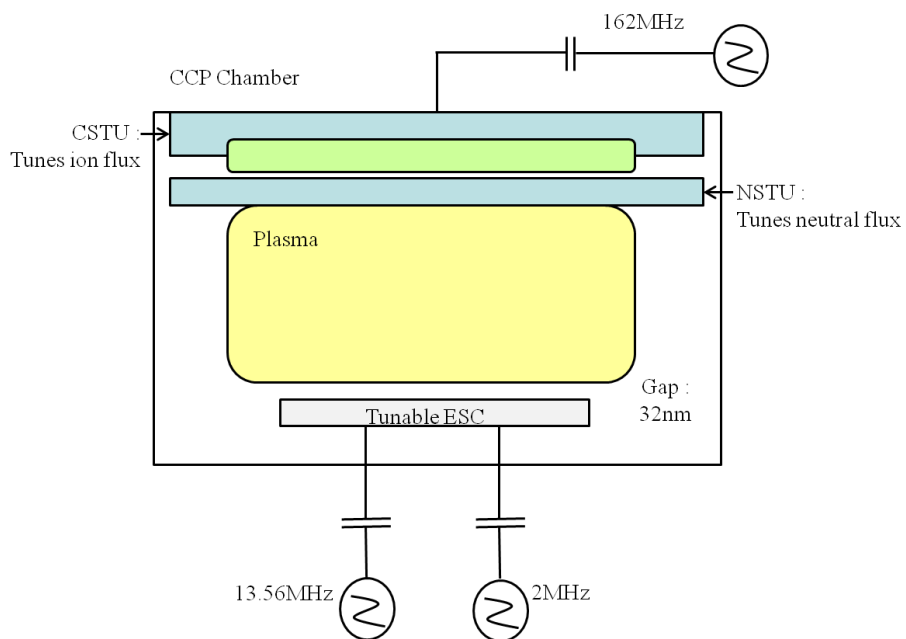


Figure 5-1. Schematic of CCP reactor employed in this chapter.

5.3. Chamber matching issues in semiconductor manufacturing

5.3.3. Chamber performance deviations in plasma etching

Figure 5-2 shows a typical example of chamber performance variations in semiconductor manufacturing. The measured etch rate of SiO₂ thin film for each chamber varies from 8.4% to 15.0% within 300mm wafer even though the average of the etch rate for each chamber is within a desired specification. This range variation of etch rate causes yield drop of wafers, which are confirmed later through electrical tests. As is shown in Fig. 5-3, the topography of the etch rate in the A-A' direction is quite different between chambers and also differs from that of the etch rate in golden chamber, which is undesirable from a device integration point of view. Thus the topography of etch rate in other chambers should be matched to the golden chamber.

The situation described in the previous paragraph generally comes from the run to run dynamics in the semiconductor manufacturing environment.^[64, 65] That is, each chamber is assembled with several thousands of parts and tens of part-kits are changed during every PM. Also, each part-kit is gradually worn out over time even after the installation. Figure 5-4 illustrates how the performance distribution of chambers changes over time. The distribution gets wider over time because chambers have experienced PM, wet cleaning, or parts swap since the installation in an end-user site. Thus, systematic methodologies of managing chambers as well as matching the performance variations will be crucial as the process window

becomes smaller in the sub-20nm semiconductor device era.

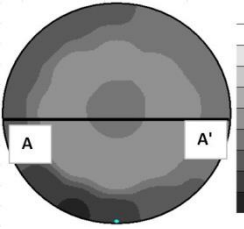
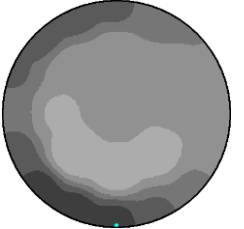
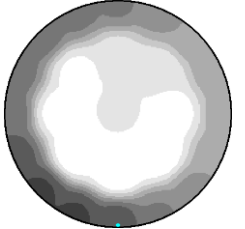
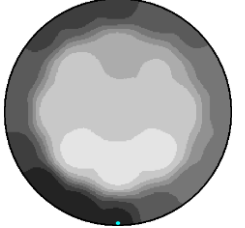
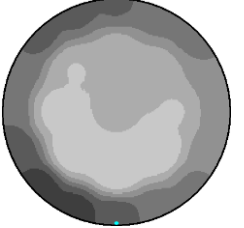
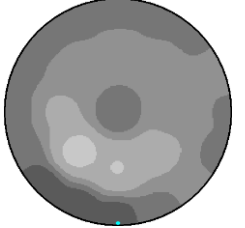
Chamber	Golden	1	2
Etch rate (Å/min) : Average (Range)	4646.7 (8.4%)	4740.2 (9.0%)	5069.3 (13.5%)
Wafer map			
Chamber	3	4	5
Etch rate (Å/min) : Average (Range)	4750.4 (15.0%)	4823.3 (10.7%)	4740.2 (9.0%)
Wafer map			

Figure 5-2. Performance differences between the golden chamber (best product yield) and other chambers in terms of etch rate maps.

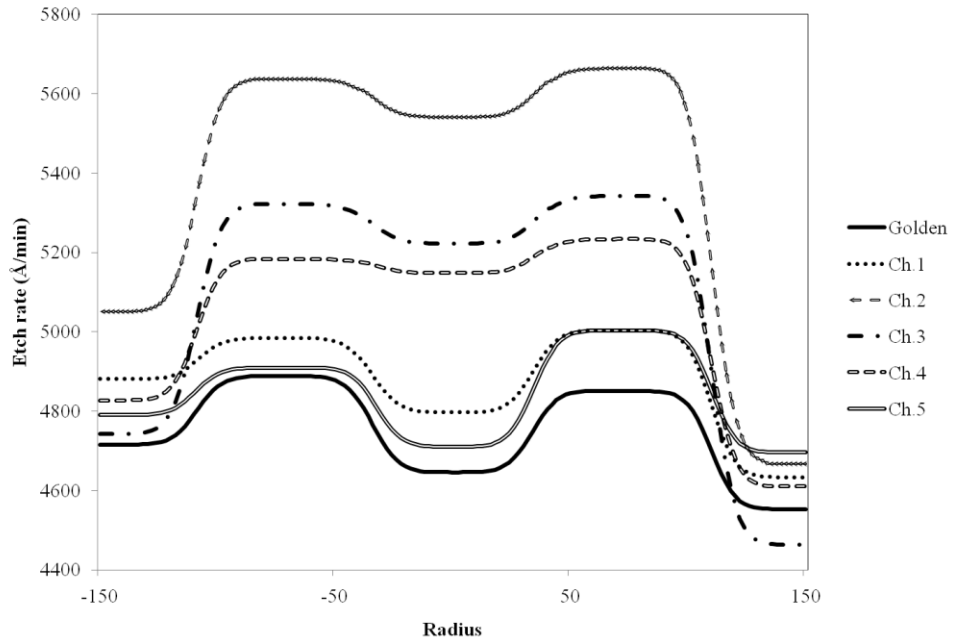


Figure 5-3. Etch rate differences between the golden chamber (best product yield) and other chambers in A-A' direction indicated in figure 5-2.

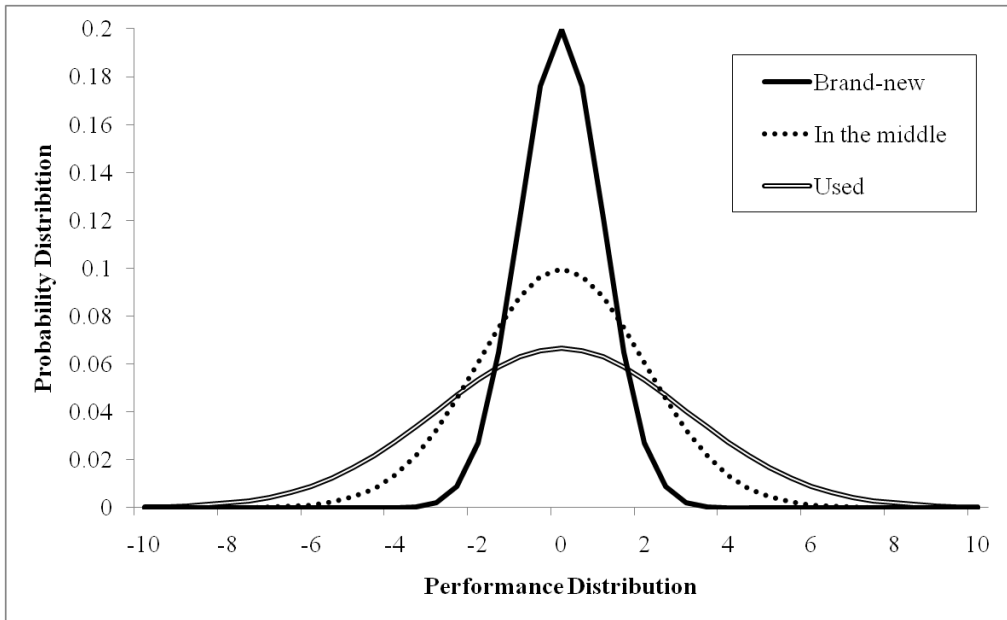


Figure 5-4. Performance distribution of chambers over time.

5.3.4. Approaches to handling chamber matching issues

Figure 5-5 shows a possible procedure to handle chamber matching issues. When chambers show variations from each other, one should first consider if the chamber states are different. If that proposition cannot be accepted, the engineers should try to find the root cause of the variations and fix the problem, which is a fault detection and classification (FDC) approach. However, if they accept the proposition, the engineers should try to find a way to match performance by controlling MVs of the equipment, which is an equipment control approach. The FDC approach is ideal but very difficult to implement because it requires monitoring sensors and detailed knowledge about hardware components. Also, if the problem comes from complicated interactions between the hardware components, it will force engineers to rely on trial and error methods. In contrast, the equipment control approach is much easier to implement because there is a step-by-step procedure for controller design like that shown in the bottom of Fig. 5-5.

This chapter focuses more on the equipment control approach than the FDC approach. This includes introduction of a few variable selection techniques using a decomposed etch rate map followed by controller design. The controlled results are confirmed with a quantitative index based on the measurement result and its usefulness is discussed.

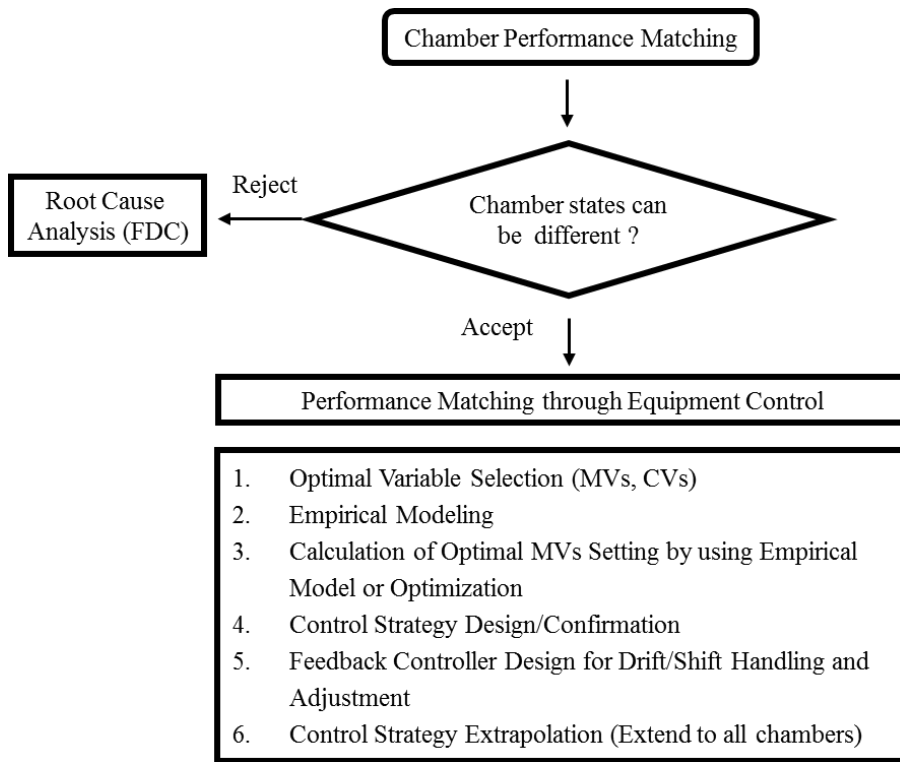


Figure 5-5. Possible procedure to handle chamber matching issues.

5.4. Brief theory overview

5.4.1. Possible MVs and CVs in plasma etching

Table 5-1 summarizes typical process variables in plasma etching, where the manipulated variables are input variables that can be changed independently with respect to time in order to control plasma and its reaction to wafer, the measured variables are those available from in-situ sensors in equipment, and the performance variables are to be optimized during operation of the process.

Among performance variables, line width or hole size of the etched pattern can be a CV because it is related to wafer yield. Other performance variables such as etch rate and its uniformity can be also a CV for an etch-back process, which is a process to etch thin film without any photolithography mask.

Since plasma is a medium connecting manipulated variables and performance variables in plasma etching, plasma parameters such as emission, electron density, and electron collision rate in Table 5-1 can be a controlled variable if we understand their relationship between manipulated and performance variables. However, due to the inherent complexity of plasma and the lack of plasma sensors, it is difficult to understand plasma parameters as a CV matching performance variables.

Table 5-1. Typical process variables in plasma etching.

Manipulated Variables	Measured Variables	Performance Variables (Controlled Variables)
Pressure	Gauge Value (Pressure,	Line Width
Power (Source/Bias)	Gas Flow, Power,	Hole Size
Gas Flow Rates	Temperature)	Etch Rate
Radial Gas Flow Ratio	Emission ([F], [CF], [Ar])	Uniformity of Etch Rate
ESC Temperature	Electron Density	Selectivity
(In/Out)	Electron Collision Rate	etc.
etc.	etc.	

5.4.2. Singular value analysis method

SVA is a powerful analytical technique that can be used to solve several important control problems such as selection of CV and MV, evaluation of the robustness of a proposed control strategy, and determination of the best multi-loop control configuration.^[41, 66]

If we consider a 2 x 2 linear steady-state process model in Eq. 5-1,

$$y = Ku + d \quad (5-1)$$

K is decomposed into its singular value decomposition like that shown in Eq. 5-2.

$$K = U\Sigma V^T = \begin{bmatrix} \cos \theta_1 & -\sin \theta_1 \\ \sin \theta_1 & \cos \theta_1 \end{bmatrix} \begin{bmatrix} \sigma_1 & 0 \\ 0 & \sigma_2 \end{bmatrix} \begin{bmatrix} \cos \theta_2 & \pm \sin \theta_2 \\ -\sin \theta_2 & \pm \cos \theta_2 \end{bmatrix}^T \quad (5-2)$$

Since U and V^T represent output and input directions of the control system and their directions are related through the singular values in the diagonal matrix Σ , the gain of the direction for each CV is determined by singular values. Thus analyzing singular values of gain matrix, K , for possible combination of MV and CV gives insight into control performance.

The insight given by the SVA method can be quantified easily by using the condition number (CN) in Eq. (5-3)^[41].

$$CN = \frac{\sigma_1}{\sigma_r} \quad (5-3)$$

Large CN means at least one direction for CV is either too weak or too strong to be effectively controlled, which can be an indication of an ill-conditioned control strategy. A well-conditioned control strategy can be found based on CN by

removing MVs or CVs of the control strategy. Two steps can be used to identify promising subsets of MVs and CVs by using CN.^[41] The first step is to arrange the singular values from largest to smallest ($\sigma_n, \sigma_{n-1}, \dots, \sigma_1$); if $\sigma_i / \sigma_{i-1} >$ a user-specific value for some $i \geq 2$, then these singular values can be neglected and at least one MV and one CV should be omitted. The second step is to generate alternative gain matrices by deleting one row and one column at a time and calculating the singular values and condition numbers. The most promising gain matrices have the smallest condition numbers.

5.4.3. Dynamic optimization techniques for multiple input multiple output control

In plasma etching, multiple CVs such as etch profile, line width, and uniformity need to be controlled simultaneously.^[21] Thus, MIMO control is more appropriate than single input single output (SISO) or multiple input single output (MISO) control. The MIMO controller can be decomposed into a series of SISO control loops (a multiloop control system). Tuning of multiloop control systems usually must be done by trial and error due to input-output interactions in the process.^[41] The principal difficulty with decomposing a multivariable system into a series of SISO control loops is that, while the dominant interactions are utilized, all other interactions are ignored. If there are interactions that are disrupting an otherwise efficient control system, then the effect of such interactions should be included in the controller design, especially for processes with many potential inputs and outputs, such as in plasma etching. In addition, if some of the CVs might be

constrained by machine and safety limitations, undesirable effects on uncontrolled outputs, and setting beyond which the unit process cost is known to increase,^[67] decomposition of the MIMO system into a series of SISO control loops may lead to lower quality control. Thus, dynamic optimization algorithms should be added for MIMO control especially in plasma etching.

The nonlinear model equation with higher order and interaction terms relating MVs and CVs, which can be developed by using experimental data from design of experiments, can be defined like that shown in Eq. 4-3.

If we obtain Eq. 4-3 by using the data from design of experiment, an optimization problem with constraints can be solved with a quadratic objective function described in Eq. 4-4 in order to obtain optimum MVs in MIMO control.^[58-60]

5.5. Controller development and recipe optimization

5.5.1. Design of MIMO controller

As is described in section 5.4.3, a MIMO controller is thought to be more appropriate than SISO or MISO controllers in plasma etching. In order to achieve a robust and feasible control result especially in the MIMO control system, selection of optimum MV to CV sets is crucial. Theoretically, perfect steady-state control is achievable if there are the same numbers of control knobs as outputs. Specifically, the preferred control strategy is a square system with each CV controlled by one MV. Plasma etching processes, however, have a large number of MVs than CVs due to the inherent complexity of the plasma. Thus, a non-square control system with more MVs than CVs generally results for the control design in plasma etching.

To design a MIMO controller, optimum CVs and MVs should be selected, which

cannot be often chosen only by using expert knowledge. To make a reasonable decision, a step-by-step procedure was followed in this thesis. As a first step, particular CVs were selected, considering the yield of wafer. The local etch rate of SiO₂ film across wafer was selected as a CV. As a second step, step change tests for individual MVs were done. Based on data from the step change test, both SVA and RGA methods were applied for selecting feasible MVs and CVs sets. With the selected CV and MV sets, an experimental model relating the CV and the MV was built by using data from the design of experiment. Considering the inherent complexity of plasma, first and second interaction terms among MVs are included in the model. The experimental model was employed for an optimization problem with constraints like that shown in Eq. 4-4 to find optimum values of each MV.

A. Determination of CVs with decomposed etch rate map

The chamber performance matching issue in this thesis comes from the topography of SiO₂ etch rate within a wafer. Figure 5-6 shows the total measurement sites of etch rate across the wafer using four directions to visualize the etch rate performance between a golden and a worst chambers. As is shown in Fig. 5-7, the etch rates between a golden and a bad chambers are clearly differentiated in terms of center, middle, and edge area. Therefore, three CVs were defined from the 25 local sites across the wafer. They are CV₁ (etch rate of site 1), CV₂ (average etch rate of the sites from 2 to 9), and CV₃ (average etch rate of the sites from 10 to 25). In addition, to qualitatively evaluate the matching performance, a performance matching index (PMI) that covers the whole behavior of the etch rate map was suggested as follows:

$$\text{PMI} = \sum_{i=1}^n w_i \frac{(ER_{i,g} - ER_{i,t})^2}{n} \quad (5-4)$$

Smaller PMI indicates better matching performance, and the value should be zero if those two chambers are perfectly matched. Starting PMIs for each chamber in Fig. 5-2 are summarized in Table 5-2. In order to select as many MVs as possible through the SVA and RGA methods, we included the average and standard deviation of SiO₂ etch rate across the wafer as additional CVs so that we could use 5 x 5 square systems when the SVA was applied.

Table 5-2. PMI for each chamber (chamber 3 was the worst chamber).

Chamber	1	2	3	4	5
PMI	21.2	31.3	100.7	59.4	45.6

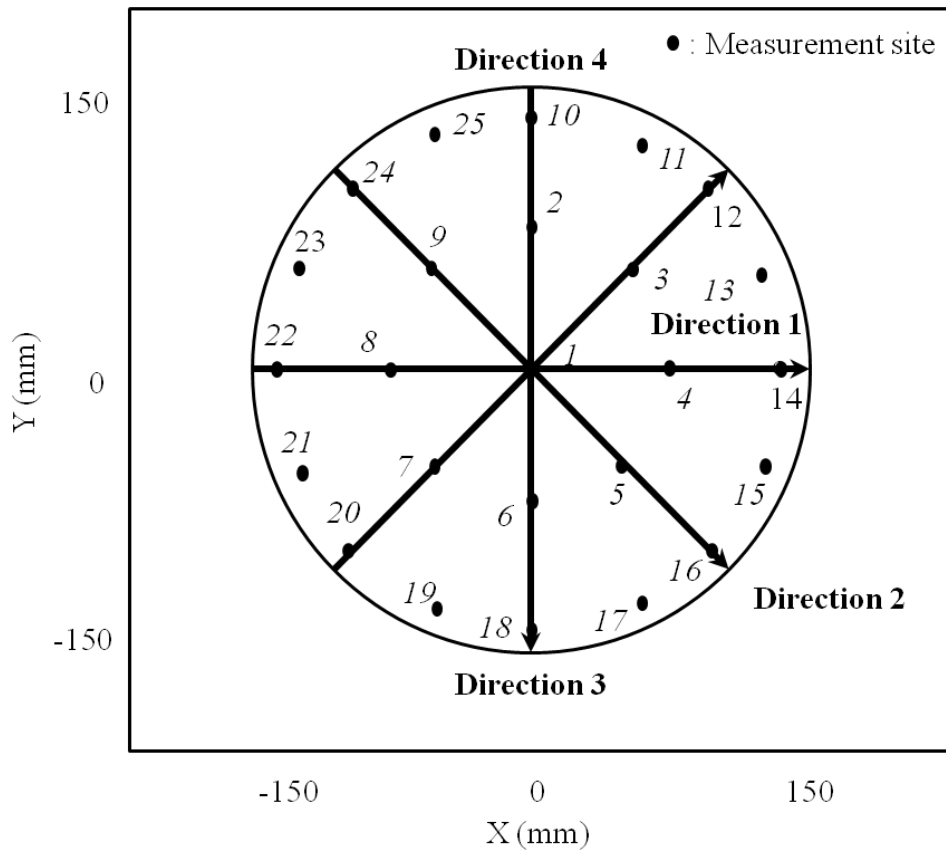


Figure 5-6. Decomposed etch rate map with four directions.

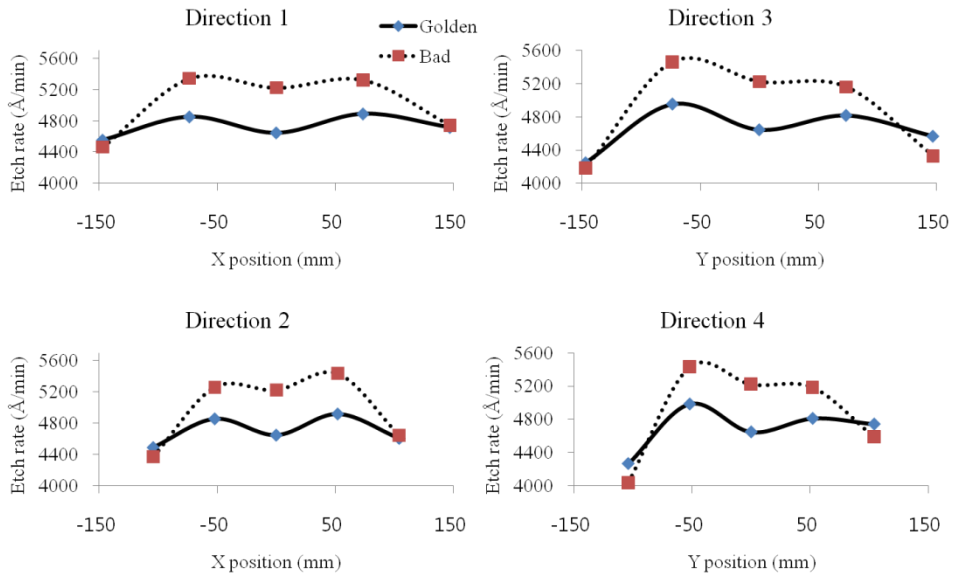


Figure 5-7. Difference of etch rate performance according to four directions in figure 5-6 between the golden and the bed chambers.

B. Preliminary determination of MVs

As a starting point, 9 MVs were selected from the recipe condition, which was recommended from expert's knowledge; 162MHz RF source power [SRC_PWR (W)], 13.56MHz RF bias power [RF1_PWR (W)], 2MHz RF bias power [RF2_PWR (W)], total pressure [pressure (mT)], C₄F₆ gas flow rate [C₄F₆ (sccm)], Ar gas flow rate [Ar (sccm)], CSTU in [CSTU-I], CSTU out [CSTU-O], and NSTU. Then, a step change test has done for these selected MVs with various ranges depending on the equipment safety limitations in order to determine steady-state relationships. After the step change test, a linear regression model was made to analyze the linearity of the MVs. Three MVs (pressure, C₄F₆, and RF1_PWR) were discarded due to their low linearity, which is based on the regression coefficient (R^2) for each model.

C. CN analysis and its verification through RGA

Table 5-3 summarizes the gain matrix with starting MVs and CVs calculated from the step change test, which are employed for the SVA and the RGA. With the gain matrix in Table 5-3, the CNs in Eq. 5-3 were calculated for every 5 x 5, 4 x 4, 3 x 3 square system. Table 5-4 summarizes the top 5 of the 4 x 4 and the 3 x 3 systems in terms of smaller CN.

Since the CN can change depending on the scaling methods,^[41] the RGA method was added for the MVs and CVs sets in Table 5-4 (a). Table 5-5 shows the RGA results for the top 5 MVs and CVs sets in Table 5-4 (a) and notifies the most promising combinations of MVs and CVs according to the pairing rules in the

RGA.^[40, 41] They are CV₁-CSTU-I or SRC PWR, CV₂-SRC PWR or CSTU-O, and CV₃-CSTU O or NSTU. These RGA results indicate that selected MVs set should include SRC PWR, CSTU-I, CSTU-O, NSTU to control the CV₁-CV₃.

Table 5-3. Raw gain matrix with 6 MVs and 5 CVs.

CVs \ MVs	SRC_PWR	RF2	Ar	CSTU-I	CSTU-O	NSTU
	Center	16.65	0.37	-0.57	-143.09	-143.78
Middle	16.34	0.42	0.45	-35.24	-57.41	741.2
Edge	2.82	1.01	8.33	193.29	265.51	261.0
Average	7.70	0.80	5.46	106.71	145.80	436.5
Stdev	1.03	-0.24	-3.42	-85.35	-107.72	60.9

Table 5-4. CN values with MVs and CVs for (a) 4 x 4 matrix and (b) 3 x 3 matrix after SVA.

(a)

Item	Selected MVs				Selected CVs	CN
1	SRC PWR	Ar	CSTU-I	CSTU-O	1 2 4 5	610
2	SRC PWR	Ar	CSTU-I	CSTU-O	1 2 3 5	759
3	SRC PWR	Ar	CSTU-I	CSTU-O	1 3 4 5	806
4	SRC PWR	Ar	CSTU-I	NSTU	1 2 3 5	962
5	SRC PWR	CSTU-I	CSTU-O	NSTU	1 3 4 5	998

(b)

Item	Selected MVs			Selected CVs	CN
1	SRC PWR	CSTU-I	CSTU-O	1 2 4	15
2	SRC PWR	CSTU-I	CSTU-O	1 2 5	17
3	SRC PWR	CSTU-I	CSTU-O	1 2 3	23
4	SRC PWR	CSTU-I	CSTU-O	2 4 5	41
5	CSTU-I	CSTU-O	NSTU	1 2 3	49

Table 5-5. RGA results with 5 top ranked MVs and CVs set in Table 5-4 (raw gain)

Variable	SRC PWR	Ar	CSUT In	*CSTU Out (**NSTU)	
#1	CV1	-0.661	-0.184	(1.518)	0.327
	CV2	0.258	0.081	-1.168	(1.830)
	CV4	(1.150)	-4.694	-4.242	8.785
	CV5	0.253	(5.797)	4.892	-9.942
#2	CV1	-0.596	-0.164	(1.746)	-0.020
	CV2	(1.039)	-0.042	-0.720	0.723
	CV3	0.270	-4.591	-4.917	(10.238)
	CV5	0.253	(5.796)	4.892	-9.941
#3	CV1	-0.694	-0.171	(2.111)	-0.246
	CV3	-0.069	-3.022	12.812	(16.924)
	CV4	(1.530)	-1.603	6.810	-5.736
	CV5	0.253	(5.797)	4.891	-0.941
#4	CV1	-0.583	-0.165	(1.731)	0.017
	CV2	(2.944)	-0.113	-0.387	-1.443
	CV3	-0.737	-0.490	0.671	(1.556)
	CV5	-0.624	(1.768)	-1.074	0.870
#5	CV1	(2.953)	4.647	-3.646	-2.954
	CV3	-0.831	-8.694	9.378	(1.147)
	CV4	-0.113	(8.653)	-9.096	1.556
	CV5	-1.009	-3.607	(4.364)	1.251

() denotes related sets between MVs and CVs, * From Top 1 to 3, ** From Top 4 to 5

D. Experimental modeling with selected MVs and CVs set

Once the optimal MVs and the corresponding CVs are determined, a MIMO control model can be developed. A theoretical model relating the MVs and CVs is desirable but since it requires fairly complete understanding of our process and plasma, a data-driven model was built by fitting a curve to the varied MV values and the corresponding CV responses using the least square method. The generalized nonlinear formulas for MIMO control are shown below:

$$\begin{aligned}y_1 &= f_1(u_1, u_2, u_3, u_4) + offset_1 \\y_2 &= f_2(u_1, u_2, u_3, u_4) + offset_2 \\y_3 &= f_3(u_1, u_2, u_3, u_4) + offset_3\end{aligned}\tag{5-7}$$

Three candidate sets of MVs are determined according to Table 5-4 (a). That is, first three sets of MVs which include CV₁ to CV₃ were selected, which are SRC PWR-Ar-CSTU I-CSTU O, SRC PWR-Ar-CSTU I-NSTU, and SRC PWR-Ar-CSTU O-NSTU (top 7 in Table 5-4 (a), which is not shown in the table because of the space).

5.5.2. Recipe optimization and chamber performance matching test

The last step is to obtain the optimum MVs setting through dynamic optimization with constraints and to finally verify matching performance through PMI. With three sets of MVs, dynamic optimization with constraints based on Table 5-6 was done. The optimization problems were solved by utilization of the *fmincon* function

in MATLAB™. Then, the prediction error for each control strategy was calculated, which is summarized in Table 5-7. Since the prediction error was the smallest value in the control strategy 2 (total 5%), the verification test was done with the second set of MVs whose optimum MVs setting are summarized in Table 5-8.

Figure 5-8 shows the verification results of the second set of MVs. The performance of the chamber closely approaches the target by applying the optimized recipe in Table 5-8. Only a 3% difference was found at center etch rate and middle etch rate respectively. Specifically, the middle etch rate between the golden and the target chambers was almost same as 4784.2 and 4767.3 A/min. In addition, the PMI was improved from 100.7 to 31.6, which is acceptable in terms of wafer yields.

Table 5-6. Constraints for each MV.

Constraints MVs	Lower bound	Upper bound
	SRC PWR (W)	380
Ar (sccm)	190	210
CSTU-I	1.0	4.0
CSTU-O	3.0	6.0
NSTU	2.0	3.0

Table 5-7. Prediction error for three control strategies.

Control CVs	Starting value (Chamber 3)	Target (Golden chamber)	1 st set of MVs	2 nd set of MVs	3 rd set of MVs
Center etch rate (A/min)	5129.9	4534.8	4800.5 (6%)	4645.8 (2%)	4534.9 (3%)
Middle etch rate (A/min)	4903.4	4784.2	4794.3 (0%)	4784.2 (3%)	4784.2 (3%)
Edge etch rate (A/min)	4654.8	4988.3	5190.2 (4%)	4988.3 (0%)	4988.3 (0%)
	Rank		3	1	2

() denotes prediction error from the target

Table 5-8. Optimized values for each MV according to control strategy.

MVs	Control	1 st set of MVs	2 nd set of MVs	3 rd set of MVs
SRC_PWR		399.9	400.0	395.5
Ar		200.0	200.1	195.8
CSTU-I		3.1	4.0	NA
CSTU-O		5.2	NA	6.0
NSTU		NA	2.3	3.0

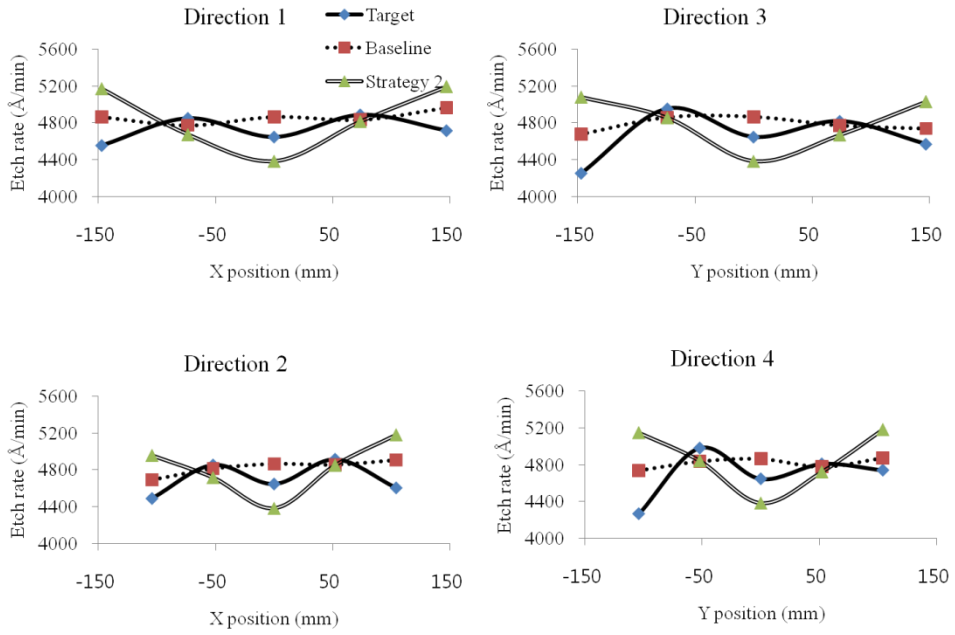


Figure 5-8. Confirmation results with the optimized condition from the second set of MVs (directions refer to figure 5-6) with PMI=31.6

5.5.3. Future aspect for robust chamber matching

Since the environment in semiconductor manufacturing is dynamic, drift or shift of chamber conditions occurs frequently.^[68, 69] For example, PM such as wet cleaning tends to causes a large shift in chamber conditions. Also, conditioning of chamber wall leads to a drift of etch rate or critical dimension in plasma etching.^[49, 55, 70] Thus, the MIMO controller should be able to handle drift and shift. In order to reflect a drift in chamber condition, the feedback control scheme using the exponentially weighted moving average filter can be incorporated into the MIMO controller. In the case of a large shift in chamber condition, recursive model update or model rebuild with the reference data set should be considered. In addition, VM could be incorporated to get more samples to enhance model update performance.^[28, 71] More studies for incorporation of those techniques should be made to maintain the performance of the MIMO controller for chamber matching in the future.

5.6. Conclusions

The equipment control approach was suggested to solve the chamber to chamber performance matching problem. The SVA and the RGA methods were employed to find the optimal sets of MVs and CVs, which could be achieved from the decomposed etch rate map. With the selected MVs and CVs, an experimental model to predict the SiO₂ etch rate has been built in a commercial CCP reactor for 300mm wafer. In order to find optimum MVs to match the etch rate performance from the worst to the golden chambers, a dynamic optimization technique with

constraints was introduced. Finally, the suggested settings of Ar flow rate, source power, CSTU-I and NSTU were applied in the worst chamber, which results in the improvement of the PMI from 100.7 to 31.6. The methodology of chamber matching will be further enhanced through a feedback control, model update, and VM in the future aspect.

CHAPTER 6 : Concluding Remarks

6.1. Conclusions

This thesis has addressed issues in cost effective plasma etch operations and solutions: sensor variable selection and utilization technique, VM to predict CD, chamber conditioning after wet cleaning, and chamber to chamber matching. All of the developed methodologies were demonstrated in semiconductor manufacturing environments.

ISR based sensor variable selection technique was introduced for handling the scaling issues from various physical properties of sensors in plasma etching and for helping to intuitively select SVs related to MVs. The ISR-based sensor variable selection technique can be integrated with relative gain array (RGA) and singular value analysis (SVA) to strengthen its usefulness in plasma etching.

Issues in implementing a robust VM for plasma etching were discussed: state-of-the art plasma sensors, effective selection of plasma sensor variables responding to individual MV, sensor data shift across PM. In order to handle selection of plasma sensor variables, ISR based sensor selection is refined by the interaction analysis from NRGAs which can reduce the number of input variables for VM. With the help of plasma sensor variables and its optimum sensor variable selection, simple linear regression methods such as MLR and PLSR are successfully applied to predict a metal line CD in plasma etching. The MAPE of the VM systems is less than 5%, which can be maintained by the cost-effective recursive coefficient update technique even under dynamic semiconductor manufacturing environments.

A systematic procedure to optimize chamber seasoning conditions with OES was suggested to address the process drift after wet cleaning in plasma etching. In order to achieve a quantitative analysis of plasma spectra without being disturbed by noises from optic systems, a self-background normalization technique is introduced. Also in order to automatically determine optimum seasoning conditions, a MIMO control strategy is applied and the optimum condition is obtained by solving the quadratic optimization problems. The suggested methodology is successfully demonstrated in a DRAM manufacturing environment suffering from a serious process drift after wet cleaning.

The equipment control approach was suggested to solve the chamber to chamber performance matching problem. The decomposed etch rate map which enables representation of etch rate profile within a wafer were introduced to design a MIMO controller with 3 CVs. With the 3 CVs, the SVA and the RGA methods were incorporated with the ISR based sensor variable selection technique to find the optimal sets of MVs and CVs. In order to find optimum MV values to match the etch rate performance from the worst to the golden chambers, an optimization problem with constraints was solved. The suggested MV values were applied to the worst chamber, which results in the improvement of the PMI from 100.7 to 31.6.

Hopefully, the proposed methodologies in this thesis will be disseminated to semiconductor manufacturers experiencing similar issues.

6.2. Future works

Extension of the well-demonstrated methodologies in this thesis will be made to other plasma related processes such as plasma enhanced-chemical vapor deposition (PE-CVD), plasma doping (PLAD), and plasma surface treatment. In addition, future works will continue in order to increase robustness of the suggested methodologies. For example, VM to predict metal CD will be further refined with the help of health check monitoring of plasma etch systems, which will be implemented with the development of an automatic health check scheduler. When it comes to chamber conditioning, an endpoint index which determines whether to continue or stop a seasoning process will be added for saving the number of NPWs more accurately. In the case of chamber matching, a FDC approach which enables finding out a root cause through automatic analysis of sensor data will be developed and compared which approaches between FDC and equipment control will be appropriate for various plasma processes. Through the comparison, case-by-case approaches will be established for effective operations. Furthermore, more sophisticated processes with photo resist pattern than the etchback process will be tried after modeling the photo resist pattern effect, in addition to the techniques shown in this thesis.

Nomenclature

a	start time of step change
b	end time of step change
d	offset
d_i	constant to minimize the error between y_i and $f_i(u_1, u_2, \dots, u_n)$
$ER_{i,g}$	etch rate of the i th site in a golden chamber
$ER_{i,t}$	etch rate of the i th site in a target chamber to be matched
\bar{e}	$(m \times n)$ steady-state error vector
$\bar{e}(i)$	$(m \times l)$ steady state error vector corresponding to the specific input $\bar{y}_{s,i}^{\text{set}}$
G	process transfer function matrix
G_s	square subsystem of G
G_R	complementary (remaining) subsystem of G
$I_{m \times n}^N$	$(m \times n)$ matrix with unity in the diagonal and zero elsewhere
K	controller transfer function matrix
K^+	Pseudo or Moore-Penrose inverse of K
T	transmittance
u	(1×2) matrix for MVs
u_j	j th manipulated variable
u_n	n th manipulated variable
w_i	weighting factor for each CV or for the i th site, which is related to the yield map across the wafer

$X_{normalization}$	normalized value of the i th sensor variable
X_i	raw value of the i th sensor variable
X_{mean}	mean of the X variables
\bar{x}_n	mean of n samples
y^*	normalized data
y_{ss}	average of steady state data points before step change
$y_+(t)$	data point at the time before and after step change
y_i	i th controlled variable
$y_{i,t}$	control target value for i th CV
y_s	output vector for the corresponding G_s
y_R	output vector for the corresponding G_R
$\bar{y}_{s,i}^{set}$	$(n \times l)$ vector with unity in the i_{th} entry and zero elsewhere
\otimes	element by element multiplication

Greek letters

A	relative gain array
A^N	non-square relative gain array
λ_{ij}	relative gain between i th controlled variable and j th manipulated variable
Σ	diagonal matrix which arranges non-negative singular values in descending order
σ	standard deviation of the X variables
σ_l	largest singular value

σ_r	smallest nonzero singular value
σ_n	standard deviation of n samples

Superscripts

N	non-square system
set	set point
T	transpose
+	Moore-Penrose pseudo-inverse
-	deviation from nominal value at steady state

Abbreviations

AEC/APC	Advanced equipment control and advanced process control
CCP	Capacitively coupled plasma
CD	Critical dimension
CN	Condition number
CPU	Central processing unit
CSTU	Charged species tuning unit
CV	Controlled variable
CVs	Controlled variables
DOE	Design of experiments
DRAM	Dynamic random access memory
EPC	Electrical parameter control
ESC	Electrostatic chuck
FinFET	Fin shaped field effect transistor

FDC	Fault detection and classification
ISMI	International SEMATECH manufacturing initiative
ISR	Integrated square response
MAPE	Mean absolute percentage error
MIMO	Multiple input multiple output
MISO	Multiple input single output
MLR	Multiple linear regression
MV	Manipulated variable
MVs	Manipulated variables
NPWs	Non-pattern wafers
NRGA	Non-square relative gain array
NSTU	Neutral species tuning unit
OES	Optical emission spectroscopy
PC	Principal component
PCA	Principal component analysis
PE-CVD	Plasma enhanced chemical vapor deposition
PLAD	Plasma doping
PLSR	Partial least squares regression
PM	Preventive maintenance
PMI	Performance matching index
PVs	Performance variables
R ²	Regression coefficient
RGA	Relative gain array
SEERS	Self-excited electron resonance spectroscopy

SEMATECH	Semiconductor manufacturing technology
SISO	Single input single output
SSE	Sum of squared errors
SVA	Singular value analysis
SVR	Support vector regression
SVs	State variables
TCAD	Technology computer aided design
VM	Virtual metrology

Literature cited

1. Moore, G.E., *Cramming more components onto integrated circuits*. Electronics, 1965. **38**(8).
2. IRC. *International Technology Roadmap for Semiconductors*. 2012; Available from: <http://www.itrs.net/Links/2012ITRS/2012Chapters/2012Overview.pdf>.
3. V. Venkatasubramanian, R.R., S. N. Kavuri, K. Yin, *A review of process fault detection and diagnosis Part III: Process history based methods*. Computers & Chemical Engineering, 2003. **27**(3): p. 327-346.
4. S. J. Qin, G.C., R. Good, J. Wang, C. A. Harrison, *Semiconductor manufacturing process control and monitoring: A fab-wide framework*. Journal of Process Control, 2006. **16**(3): p. 179-191.
5. B. M. Wise, N.B.G., *The process chemometrics approach to process monitoring and fault detection*. Journal of Process Control, 1996. **6**(6): p. 329-348.
6. J. F. MacGregor, T.K., *Statistical process control of multivariate processes*. Control Engineering Practice, 1995. **3**(3): p. 403-414.
7. Jackson, J.E., *A User's Guide to Principal Components*. 1991, New York: Wiley Interscience.
8. Qin, S.J., *Statistical process monitoring: Basics and beyond*. Journal of Chemometrics, 2003. **17**(8-9): p. 408-502.
9. P. Nomikos, J.F.M., *Multivariate SPC charts for monitoring batch*

- processes*. Technometrics, 1995. **37**(1): p. 41-59.
10. H. H. Yue, S.J.Q., R. J. Markle, C. Nauert, M. Gatto, *Fault detection of plasma etchers using optical emission spectra*. IEEE Transactions on Semiconductor Manufacturing, 2000. **13**(3): p. 374-385.
 11. T. Sonderman, C.B. *Automated precision manufacturing: A key to yield in semiconductor manufacturing*. in *AIChE annual meeting*. 2004. Austin, TX.
 12. Spanos, C.J. *Coping with variability in semiconductor manufacturing*. in *AIChE annual meeting*. 2004. Austin, TX.
 13. R. D. Braatz, R.C.A., E. G. Seebauer, T. O. Drews, E. Rusli, M. Karulkar, F. Xue, Y. Qin, M. Y. L. Jung, R. Gunawan, *A multiscale systems approach to microelectronic processes*. Computers & Chemical Engineering, 2006. **30**(10-12): p. 1643-1656.
 14. Edgar, T.F. *Batch process control: Will semiconductor manufacturing lead the way?* in *AIChE Annual Meeting*. 2004. Austin, TX.
 15. I. G. Kevrekidis, C.W.G., G. Hummer, *Equation-free: The computer aided analysis of complex multiscale systems*. AIChE journal, 2004. **50**(7): p. 1346-1355.
 16. K. H. Baek, Y.J., G. J. Min, C. Kang, H. K. Cho, J. T. Moon, *Chamber maintenance and fault detection technique for a gate etch process via self-excited electron resonance spectroscopy*. Journal of Vacuum Science and Technology B, 2005. **23**(1): p. 125-129.
 17. R. Chen, H.H., C. J. Spanos, M. Gatto, *Plasma etch modeling using optical emission spectroscopy*. Journal of Vacuum Science and Technology A, 1996. **14**(3): p. 1901-1906.

18. M. Klick, W.R., M. Kammeyer, *Plasma diagnostics in rf discharges using nonlinear and resonance effects*. Japanese Journal of Applied Physics Part 1, 1997. **36**(7B): p. 4625-4631.
19. H. M. Park, D.S.G., J. W. Grizzle, *Sensor fault detection in etch based on broadband rf signal observation*. Journal of Vacuum Science and Technology A, 2003. **21**(3): p. 814-824.
20. Sobolewski, M.A., *Real-time, noninvasive monitoring of ion energy and ion current at a wafer surface during plasma etching*. Journal of Vacuum Science and Technology A, 2006. **24**(5): p. 1892-1905.
21. M. A. Lieberman, A.J.L., *Principles of Plasma Discharges and Materials Processing*. 2005, New Jersey: John Wiley & Sons, Inc.
22. J. W. Coburn, M.C., *Optical emission spectroscopy of reactive plasmas: A method for correlating emission intensities to reactive particle density*. Journal of Applied Physics, 1980. **51**(6): p. 3134-3136.
23. E. Semmler, P.A., A. Keudell, *Heating of a dual frequency capacitively coupled plasma via plasma series resonance*. Plasma Sources Science and Technology, 2007. **16**(4): p. 839-848.
24. Klick, M., *Nonlinearity of the radio-frequency sheath*. Journal of Applied Physics, 1996. **79**(7): p. 3445-3452.
25. Jolliffe, I.T., *Principal component analysis*. 2nd Edition ed. 2002, New York: Springer.
26. S. Wold, K.E., P. Geladi, *Principal component analysis*. Chemometrics and Intelligent Laboratory Systems, 1987. **2**(1-3): p. 37-52.
27. P. Kang, H.J.L., S. Cho, D. Kim, J. Park, C. K. Park, S. Doh, *A virtual*

- metrology system for semiconductor manufacturing*. Expert Systems with Applications, 2009. **36**: p. 12554-12561.
28. A. A. Khan, J.R.M., D. M. Tilbury, *Virtual metrology and feedback control for semiconductor manufacturing processes using recursive partial least squares*. Journal of Process Control, 2008. **18**(10): p. 961-974.
 29. P. Chen, S.W., J. Lin, F. Ko, H. Lo, J. Wang, C. H. Yu. *Virtual metrology: a solution for wafer to wafer advanced process control*. in *International Symposium on Semiconductor Manufacturing*. 2005. San Jose, CA, USA.
 30. M. H. Hung, T.H.L., F. T. Cheng, R. C. Lin, *A novel virtual metrology scheme for predicting CVD thickness in semiconductor manufacturing*. IEEE/ASME Transactions on Mechatronics, 2007. **12**(3): p. 308-316.
 31. S. A. Lynn, J.V.R., E. Ragnoli, S. Mcloone, N. MacGearailt. *Virtual metrology for plasma etch using tool variables*. in *IEEE/SEMI Advanced Semiconductor Manufacturing Conference*. 2009. Berlin, Germany.
 32. D. Zeng, C.J.S., *Virtual metrology modelling for plasma etch operations*. IEEE Transactions on Semiconductor Manufacturing, 2009. **22**(4): p. 419-431.
 33. S. I. Imai, M.K., *Prevention of copper interconnection failure in system on chip using virtual metrology*. IEEE Transactions on Semiconductor Manufacturing, 2009. **22**(4): p. 432-437.
 34. V. Vitale, W.A., A. Hunter, I. Iliopoulos, N. Kroupnova, A. Yanovich, N. Merry. *Use of virtual metrology for in-situ visualization of thermal uniformity and handoff adjustment in RTP critical anneals*. in *IEEE/SEMI Advanced Semiconductor Manufacturing Conference*. 2008. Cambridge,

MA, USA.

35. P. Kang, D.K., H. J. Lee, S. Doh, S. Cho, *Virtual metrology for run-to-run control in semiconductor manufacturing*. Expert Systems with Applications, 2011. **38**: p. 2508-2522.
36. D. White, B.G., A. Gower, D. Boning, H. Chen, H. Sawin, T. Dalton, *Low open-area endpoint detection using a PCA-based T2 statistics and Q statistic on optical emission spectroscopy measurements*. IEEE Transactions on Semiconductor Manufacturing, 2000. **13**(2): p. 193-207.
37. B. M. Wise, N.B.G., S. W. Butler, D. D. White Jr, G. G. Barna, *A comparison of principal component analysis, multiway principal component analysis, trilinear decomposition and parallel factor analysis for fault detection in a semiconductor etch processes*. Journal of Chemometrics, 1999. **13**: p. 379-396.
38. T. H. Lin, F.T.C., A. J. Ye, W. M. Wu, M. H. Hung. *A novel key variable sifting algorithm for virtual metrology*. in *IEEE International Conference on Robotics and Automation*. 2008. Pasadena, CA, USA.
39. Y. J. Kim, K.H.B., Y. J. Kim, S. W. Choi, W. S. Han. *In-situ plasma monitoring and virtual metrology via SEERS in dielectric etch*. in *8th European AEC/APC conference*. 2007. Dresden, Germany.
40. Bristol, E.H., *On a new measure of interactions for multivariable process control*. IEEE Transactions on Automatic Control, 1966. **AC-11**: p. 133-135.
41. D. E. Seborg, T.F.E., D. A. Mellichamp, *Process Dynamics and Control*. 2003, New York: Wiley.

42. J. Chang, C.C.Y., *The relative gain for non-square multivariable systems*. Chemical Engineering Science, 1990. **45**(5): p. 1309-1323.
43. G. Spitzlsperger, C.S., G. Ernst, H. Strasser, M. Speil, *Fault detection for a Via etch process using adaptive multivariate methods*. IEEE Transactions on Semiconductor Manufacturing, 2005. **18**(4): p. 528-533.
44. M. C. Johannesmeyer, A.S., D. E. Serborg, *Pattern matching in historical data*. AIChE journal, 2002. **48**: p. 2022-2038.
45. A. J. Smola, B.S., *A tutorial on support vector regression*. Statistics and computing, 2004. **14**(3): p. 199-222.
46. B. S. Dayal, J.F.M., *Recursive exponentially weighted PLS and its applications to adaptive control and prediction*. Journal of Process Control, 1997. **7**(3): p. 169-179.
47. K. Helland, H.E.B., O. S. Borgen, H. Martens, *Recursive algorithm for partial least squares regression*. Chemometrics and Intelligent Laboratory Systems, 1992. **14**(1-3): p. 129-137.
48. Qin, S.J., *Recursive PLS algorithms for adaptive data modeling*. Computers & Chemical Engineering, 1998. **22**(4-5): p. 503-514.
49. S. Xu, T.L., D. Podlesnik, *Wall-dependent etching characteristics of organic antireflection coating O₂+halogen/hydrogen halide plasma*. Journal of Vacuum Science and Technology A, 2001. **19**(6): p. 2893-2899.
50. J. A. O'Neill, J.S., *Role of the chamber wall in low-pressure high-density etching plasmas*. Journal of Applied Physics, 1995. **77**(2): p. 497-504.
51. P.I. Klimecky, J.W.G., L. F. Terry *Compensation for transient chamber wall condition using real-time plasma density feedback control in an*

- inductively coupled plasma etcher*. Journal of Vacuum Science and Technology A, 2003. **21**(3): p. 706-717.
52. S. J. Ullal, A.R.G., E. Edelberg, L. Braly, V. Vahedi, E. S. Aydil, *Effect of chamber wall conditions on Cl and Cl₂ concentrations in an ICP reactor*. Journal of Vacuum Science and Technology A, 2002. **20**(1): p. 43-52.
53. Donnelly, V.M., *A simple optical emission method for measuring percent dissociations of feed gases in plasmas: Application to Cl₂ in a high-density helical resonator plasma*. Journal of Vacuum Science and Technology A, 1996. **14**(3): p. 1076-1087.
54. G. I. Font, I.D.B., and J. Balakrishnan, *Effects of wall recombination on the etch rate and plasma composition of an etch reactor*. Journal of Vacuum Science and Technology A, 1998. **16**(4): p. 2057-2064.
55. S. J. Ullal, H.S., J. Daugherty, V. Vahedi, E. S. Aydil, *Maintaining reproducible plasma reactor wall conditions: SF₆ plasma cleaning of films deposited on chamber wall during Cl₂/O₂ plasma etching of Si*. Journal of Vacuum Science and Technology A, 2002. **20**(4): p. 1195-1201.
56. S. Park, K.H.B., Y. Kim, H. K. Lee, S. Jeong, G. Seong, *Plasma apparatus having a controller for controlling a plasma chamber and methods for controlling the plasma apparatus*. 2011, Samsung Electronics Co., Ltd.
57. Prism Research Glass, I. *Technical Specifications*. 2011; Available from: http://www.prismresearchglass.com/magento/index.php/technical_specifications.
58. T. F. Edgar, D.M.H., L. S. Lasdon, *Optimization of chemical processes*. 2001, New York: McGraw-Hill.

59. H. Lee, A.R., D. Prager, K. A. Bandy, E. Meyette, R. Sundararajan, A. Viswanathan, A. Yamashita, M. Funk. *Advanced profile control and the impact of sidewall angle at gate etch for critical nodes*. in *SPIE*. 2008.
60. B. R. Parkinson, H.L., M. Funk, D. Prager, A. Yamashita, R. Sundararajan, T. F. Edgar, *Addressing dynamic process changes in high volume plasma etch manufacturing by using multivariate process control*. *IEEE Transactions on Semiconductor Manufacturing*, 2010. **23**.
61. K. H. Baek, K.P.H., G. Choi, H. K. Kang, E. S. Jung, K. Song, C. Han, T. F. Edgar, *Multiple input multiple output controller design to match chamber performance in plasma etching for semiconductor manufacturing*. *Journal of Vacuum Science and Technology B*, 2013. **31**(6).
62. K. H. Baek, B.C., M. Carbery, J. Y. Woo, T. S. Lee, H. S. An, Y. Koo, C. Han, S. Han, Y. Kim, S. W. Choi, W. Han. *Process and chamber health monitoring of plasma enhanced Ti deposition process through high performance VI-probe*. in *International Symposium on Semiconductor Manufacturing*. 2007.
63. M. Tesauro, G.R., *Instrument wafers enable etch chamber matching*. *Solid State Technology*, 2008. **51**.
64. M. Zhou, M.D.J., *Modeling, Analysis, Simulation, Scheduling, and Control of Semiconductor Manufacturing Systems: A Petri Net Approach*. *IEEE Transactions on Semiconductor Manufacturing*, 1998. **11**(3): p. 333-357.
65. J. A. Mullins, W.J.C., A. D. Stock. *An evaluation of model predictive control in run to run processing in semiconductor manufacturing*. in *SPIE*. 1997.

66. H. Lau, J.A., K. F. Jensen, *Synthesis of control structures by singular value analysis:dynamics measures of sensitivity and interaction*. AIChE journal, 1985. **31**.
67. A. E. Gower-Hall, D.S.B., *Model-based uniformity control for epitaxial silicon deposition*. IEEE Transactions on Semiconductor Manufacturing, 2002. **15**(3): p. 295-309.
68. N. Gallagher, B.W., S. Butler, D. white, G. Barna. *Development and benchmarking of multivariate statistical process control tools for a semiconductor etch process:Improving robustness through model updating*. in *IFAC ADCHEM*. 1997.
69. K. Chamness, T.F.E. *Diagnostics of plasma etch:PCA with adaptive centering and scaling*. in *Sematech AEC/APC Symposium XV*. 2003.
70. S. Xu, Z.W.S., X. Y. Qian, J. P. Holland, D. Podlesnik, *Characteristics and mechanism of etch process sensitivity to chamber surface condition*. Journal of Vacuum Science and Technology B, 2001. **19**(1): p. 166-171.
71. Y. J. Chang, Y.K., C. L. Hsu, C. T. Chang, T. Y. Chan. *Virtual metrology technique for semiconductor manufacturing*. in *Proceedings of the International Joint Conference on Neural Networks*. 2006.

Abstract in Korean (요 약)

수십 년 동안 반도체 산업은 기술의 빠른 발전에 기인하여 급속하게 진보되어 왔다. 지속적인 반도체 크기의 축소는 20 나노 이하 급의 반도체 시대를 열었고, 이에 따라서 멀티코어의 마이크로프로세서, 수백기가 바이트 급의 다양한 메모리 반도체를 가능하게 하였다. 이러한 기술의 진보는 무어의 법칙에 의하여 주도되었고, 그 법칙의 유효성은 최근의 20나노 이하 급 반도체 시대까지 정확하게 증명되었다. 그러나, 물질 및 패터닝 기술의 물리적인 어려움 때문에 10나노 이하의 반도체 크기 축소는 어려워 보이며, 이에 대한 대안으로 무어의 법칙 이후의 컨셉에 대하여 2007년 처음 논의 되었다. 이것은 반도체 크기의 축소가 아닌 동등한 성능의 개선을 새로운 공정 기술의 적용, 칩 및 시스템 레벨에서의 디자인 혁신, 450mm 웨이퍼로의 생산 이전, 그리고 실시간 모니터링 및 컨트롤을 통한 비용 절감 생산 등을 통하여 이룩하는 것이다. 반도체 제조는 다양한 공정들로 구성되어 있다. 가령 포토리소그래피, 식각, 확산, 이온 주입, 막 증착, 세정 그리고 화학적 기계적 연마 등이다. 이들 공정 중에서 플라즈마와 연관된 공정은 전체 제조 스텝 중 30% 이상을 차지하고 있고, 특히 플라즈마 식각은 반도체 제조를 위한 플라즈마 설비 기술의 진보를 이끌고 있다.

플라즈마 식각에서의 모니터링 및 컨트롤을 통한 비용 절감 생산 기술은 플라즈마의 본질적인 복잡함, 플라즈마 센서의 부족, 증착 및 포토리

소그래피와 연관된 문제 발생 등의 이유로, 반도체 제조에서의 코어 공정임에도 불구하고, 지금까지 크게 진보하지 못해왔다.

본 논문에서는 플라즈마 식각에서의 비용 절감 생산을 위하여 문제점 그리고 그것에 대한 해결 방법을 제시하고자 한다. 특히 센서 변수 선정 및 활용 기술, 가상 계측 시스템, 챔버 세정 이후의 컨디셔닝 공정 최적화, 챔버간의 성능 매칭 등이다. 본 논문에서 개발된 방법들은 실제 반도체 제조 생산 라인에서 그 효용성을 검증 받았다.

새롭게 제시된 센서 변수 선정 기술은, 플라즈마 식각에서의 다양한 센서들의 물리적인 단위 차이에서 발생하는 문제, 그리고 직관적으로 공정 변수와 연관된 센서 변수를 선정할 수 있도록 하는 것을 특징으로 한다. 이 기술은 기존의 relative gain array 및 singular value analysis 등의 방법과 연결되어 활용 가능함으로써, 그 유용성을 극대화 할 수 있다.

플라즈마 식각에서의 가상 계측 시스템 구현의 문제점 역시 논의되었다. 이들은, 최신식의 플라즈마 센서들, 개별적인 공정 변수와 연결된 플라즈마 센서 선정, 예방 정비 후 발생하는 센서 변수 값의 변동 등이다. 플라즈마 센서들의 효과적인 선정을 위해서 본 논문에서 제시된 새로운 센서 변수 선정 방법이 활용되었고, 이 방법에 의하여 선정된 센서들은 다시 non-square relative gain array 방법으로 재 검증 되었다. 이를 통하여 가상 계측 시스템을 위한 입력 변수 수를 줄일 수 있었고, 이러한 효과적인 입력 변수 선정 덕분에, 간단한 회귀 분석법(multiple

linear regression, partial least squares regression)으로도 가상 계측 시스템의 절대 예측 오차를 5% 미만으로 유지할 수 있었다. 또한 반도체 제조의 다이내믹스에 기인된 노이즈 팩터는 순환적인 계수 갱신법을 적용하여, 가상 계측 시스템의 절대 예측 오차를 5% 미만으로 지속할 수 있었다.

광 방출 분광기를 활용하여 체계적으로 챔버 컨디셔닝 조건을 만드는 방법은, 챔버 세정 후 발생하는 공정 결과 변동 문제를 해결하기 위하여 제시되었다. 플라즈마로부터의 광 방출을 정량적으로 분석 가능하게 하기 위하여 새로운 시그널 처리 방법이 제시되었으며, 자동적으로 최적 챔버 컨디셔닝 조건을 만들기 위하여 다중 입력 다중 출력의 컨트롤러를 디자인 하였다. 제시된 방법에 의하여 최적화된 챔버 컨디셔닝 조건을 적용함으로써, 챔버 세정 후 발생한 공정 결과 변동 문제를 완벽하게 해결할 수 있었다.

챔버간의 성능 차이를 맞추기 위하여 설비 제어 접근법이 제시되었다. 다중 입력 다중 출력 컨트롤러 디자인이 가능하도록 decomposed etch rate map이 제시되었고, 이를 통하여 웨이퍼 내의 식각률 프로파일을 3개의 변수로 대표할 수 있었다. 최적의 변수 선정은 본 논문에서 제시된 센서 변수 선정 방법이 적용되었고, 최적의 공정 조건은 제한이 있는 최적화 문제를 계산함으로써, 얻을 수 있었다. 최적 공정 조건 적용 결과 최악의 챔버 성능이 최고로 좋은 챔버의 성능에 근접하였고, 이것은 성능 매칭 인덱스로 정량적으로 검증되었다.

본 논문에서 제시된 방법들이 비슷한 문제들로 어려움을 겪고 있는 반도체 제조사들에게 전파되어 그들의 문제 해결에 도움이 되기를 기대한다.

주요어: 플라즈마 식각, 변수 선정, 가상 계측, 다중 입력 다중 출력 컨트롤러, 챔버 컨디셔닝, 챔버 매칭

학번: 2010-30250

성명: 백 계 현